School of Information Technology and
Engineering at the ADA University

School of Engineering and Applied Science
at the George Washington University

ENHANCING POWER GRID RESILIENCE TO EARTHQUAKES USING DEFENSIVE ALGORITHM

A Thesis
Presented to the Graduate Program of Electrical and Power Engineering
of the School of Information Technology and Engineering
ADA University

In Partial Fulfillment
of the Requirements for the Degree
Master of Science in Electrical and Power Engineering
ADA University

By
Aishat Seyidova

December, 2024

THESIS ACCEPTANCE

This Thesis by: Aishat Seyidova
Entitled: *Enhancing Power Grid Resilience to Earthquakes Using Defensive Algorithm*

has been approved as meeting the requirement for the Degree of Master of Science in Electrical and Power Engineering of the School of Information Technology and Engineering, ADA University.

Approved:

(Adviser)	(Date)
(Program Director)	(Date)
(Dean)	(Date)

ABSTRACT

Enhancing power resilience of electrical systems to natural hazards, such as earthquakes, windstorms, floods,etc. is crucial for avoiding disruptions in global infrastructures as well as for maintaining economic stability and public welfare. Earthquakes are one of the corruptive hazards that refer to High Impact Low Probability (HILP) events and can severely damage power stations, leading to massive outages and cascading failures. Thus, this research aims to raising the issue via introducing an innovative approach such as utilising a defensive islanding algorithm to enhance the seismic resilience of power networks. The approach encompasses different analytical tools, including but not limited to fragility curve & load flow analysis, spectral clustering, a Severity Risk Index employment, and Monte Carlo simulations to establish a comprehensive framework for risk assessment. Fragility curves are located at the epicenter when it comes to assesing the likelihood of component failure across various earthquake intensities and also it provides a comprehensive insight into system vulnerabilities. Peak Ground Acceleration (PGA) plays the role of the key variable for our analysis. Multiple earthquake scenarios are generated by Monte Carlo simulations to cover the stochastic characteristics of seismic hazards and their possible impacts on the electrical grid. A Severity Risk Index identifies the most susceptible branches and essential components of the network that may lead to power outages. For this introductory research of applying defensive islanding particularly to earthquakes, parameters mentioned above are more that sufficient for formulating a precise and well-defined strategy. Defensive islanding, which presumably divides the electrical system into autonomous sections, so called "islands" is a central component of this technique. It helps to mitigate interruptions during a seismic event or series of similar hazards. Additionally, spectral clustering is selected at the most recent & eficient techniques to improve the islanding process, making sure that each island is resilient and able to feed substantial loads. Overall, the strategy is helpful due to the fact that it enhances the operational capacity of the system not only during a hazardous event but also following that event. It divides the zones that are under higher risk and maintains the stability of unaffected areas. The methodology is defined through the test case study named IEEE 24-bus system which can also be reffered as "Reliability Test". The MATPOWER library is mainly used for incorporating load flow analysis, evaluating the system's initial as well as subsequent characteristics. There are numerous variables analysed through MATPOWER: voltage levels, phase angles, power losses, etc. Simulation results highlight the fact that the strategy ultimately reduces the probability of cascade failures and improves the system's resistance to natural and sudden disturbances. The paper emphasizes the vital significance of resilience strategies in protecting fundamental loads during natural catastrophes, thereby providing necessary data to utility operators, researches and policymakers. The implemented strategy concentrates on a substantional improvement in the planning of seismic resilience for power systems. The research presents a pragmatic and dynamic methodology for mitigating earthquake hazards through the integration of probabilistic risk assessment and sophisticated network optimisation algorithms. This paper not only addresses power grid resilience but also offers effective ways for improving infrastructure stability and facilitating long-term recovery after seismic occurrences. Additionally, the study provides further room for improvement by incorporating real-time monitoring systems, IoT technology and machine learning models for early detection of natural hazardous events.

Keywords: high impact low probability (HILP), natural hazards, defensive islanding, power resilience, seismic events, fragility curves, peak ground acceleration (PGA), spectral clustering

TABLE OF CONTENTS

LIST OF FIGURES

LIST OF TABLES

LIST OF ABBREVIATIONS

Abbreviation	Explanation
FC	Fragility Curve
HILP	High Impact Low Probability
MCS	Monte Carlo Simulation
PGA	Peak Ground Acceleration
SRI	Severity Risk Index

CHAPTER ONE

INTRODUCTION

A. Problem Statement and Research Motivation

High Impact Low Probability events have the capacity to shake the electric power infrastructure, causing damage that can be either temporary or permanent. Among such HILP events, earthquakes are particularly destructive.[4] Being mostly unpredictable, seismic activities can lead to extensive damage to power generation plants, transmission lines, substations and distribution systems.[2] The ground shaking, and surface rupture associated with earthquakes can topple transmission towers, fracture underground cables, and cause transformers to malfunction. [6] In severe cases, this damage can result in widespread and prolonged power outages, complicating recovery efforts and impacting emergency services, businesses, and residents.

Over the past few years, several major earthquakes caused extensive destruction worldwide, impacting not only human lives but also critical infrastructure, particularly power systems. In 2020, the Aegean Sea earthquake with magnitude 7.0 affected Greece and Turkey, resulting in 119 deaths and severe damage to infrastructure, particularly in Izmir, Turkey.[5] The earthquake resulted in power outages affecting approximately 500,000 customers and inflicted economic losses estimated at $400 million.[5] In 2021, the Haiti earthquake with magnitude 7.2 resulted in over 2,200 fatalities and devastated the country's power grid, leaving more than 1.5 million people without electricity. The destruction of power infrastructure exacerbated challenges in healthcare, housing, and transportation, with economic losses estimated at $1.5 billion. The 2023 earthquake in Turkey [29] and Syria [5] with magnitude 7.8 was particularly devastating, claiming over 350,000 lives and causing $34 billion in damages. Approximately 3 million customers were left without power as power plants and industrial facilities suffered extensive destruction, severely impacting the energy supply and economic stability of the region. Most recently, the 2024 Noto Peninsula earthquake [5] in Japan with magnitude 7.5 resulted in structural damage and destruction of power plants, leading to power outages affecting approximately 2 million customers and economic losses totaling $6 billion. Figure 1 shows statistics on the number of earthquakes with magnitude >5 on a yearly basis worldwide. From the chart we can say that the number of significant earthquakes (magnitude>5) each year suggests that earthquakes are a persistent natural hazard. The peak in 2021 shows that years with higher seismic activity can harm existing infrastructure, making ongoing resilience planning essential.[58]

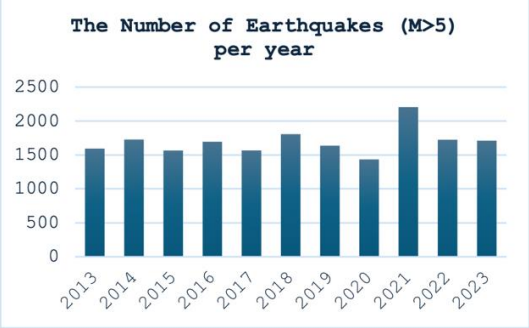

Figure 1. 2013-2023 seismic activity worldwide [58]

Notwithstanding significant efforts in seismic retrofitting and early warning systems, the ongoing susceptibility of power systems to seismic threats continues to be a concern particularly knowing that the number of HILP events is getting increased on daily basis causing massive disruptions. Current methodologies predominantly emphasize fortifying infrastructure, such the reinforcement of transmission towers and substations, or the deployment of distributed energy resources (DERs) for localized resilience. Although these procedures are essential, they frequently lack integration with dynamic, real-time mitigation solutions capable of adapting to the changing nature of seismic events.

This gap requires the creation of novel frameworks that integrate vulnerability assessments with proactive operational strategies, such as defensive islanding, to improve overall system resilience. In contrast to conventional hardening strategies that concentrate on fortifying individual elements, defensive islanding tackles the systematic characteristics of power systems. By grouping power network into separate independent elements, it firstly prioritizes critical loads which needed to be isolated in a fastest and most efficient way. In addition, this method takes into consideration further actions that need to be taken such as load shedding, real-time monitoring which corresponds to a more sustainable and safe solution.

Thus, this study's main goal is to demonstrate the advantages as well as practicality of choosen strategy in order to motivate scholars to contribute to research and innovation in power system resilience. Therefore, it becomes obvious that this project aims to connect theoretical research with practice by making an emphasis to real-world applicability, thereby stimulating a more resilient energy future.

B. Terminology Definition

Throughout this paper, certain terminology will be used to guarantee a thorough understanding of complex methodologies and techniques:

- Power Grid Resilience: The ability of an electric power system to predict, withstand and reduce the magnitude of disruptive events.

- Defensive Islanding: A protection method that is responsible for maintaining the stability of the power grid by dividing one network into smaller independent islands as soon as it detects the vulnerability in the grid.

- Spectral Clustering: A mathematical methodology to classify network components into clusters according to given criteria, such as susceptibility or operational limitations.

- Fragility Curves: A key representation demonstrating the probabilistic damage or failure of the power components based on the key inputs characterizing any HILP event.

- Peak Ground Acceleration (PGA): a key metric in seismic analysis to determine fragility curves.

- Monte Carlo Simulation (MCS): A computational technique employing random sampling to simulate uncertainty and variability in earthquake scenarios, facilitating comprehensive risk assessments.

- Severity Risk Index (SRI): A quantitative measure that assesses the likelihood of sequential failures in a power network subjected to seismic stress.

C. Importance of the Research

Robustness of power grids to seismic disasters is not just a technological problem, but a societal imperative. Reliable electricity supply is fundamental to modern economies, facilitating the operation of health services, communication networks, and industrial activities during crises.
The increasing frequency and intensity of seismic events require a fundamental change in the approach to resilience.
This study demonstrates a new way to enhance the resilience of power grids using a protective isolation strategy. The proposed framework provides a comprehensive method for seismic hazard management by integrating fragility curves, Monte Carlo simulations, spectral clustering, and load flow analysis. Protective isolation is important for its ability to proactively isolate vulnerable network segments, thereby reducing cascading failures and protecting essential services.The use of this methodology in the IEEE 24-bus system, a recognized benchmark in power system analysis, facilitates a comprehensive assessment of its performance.The results indicate that proactive islanding solutions markedly diminish system-wide disturbances and expedite recovery durations.
This research addresses a significant gap by integrating infrastructure-based hardening measures with operational resilience techniques, offering a flexible and responsive approach to seismic threats.
The study provides utility operators, policymakers, and researchers with practical insights for cost-effective resilience planning. By emphasizing the relationship between infrastructure vulnerabilities and operational strategies, it highlights the necessity of incorporating predictive modeling and real-time decision-making into resilience frameworks. The study's focus on spectral clustering for island creation provides a new approach to designing grid topology to endure seismic disturbances.
This research aids global initiatives in disaster risk mitigation and sustainable development. By maintaining the continuity of critical services during seismic occurrences, it bolsters the resilience goals established in international frameworks like the Sendai Framework for Disaster Risk Reduction. Furthermore, the study's emphasis on reducing economic and social repercussions corresponds with the United Nations Sustainable Development Goals, namely Goal 9 (Industry, Innovation, and Infrastructure) and Goal 11 (Sustainable Cities and Communities).

D. Constraints of the Research

The study enhances the comprehension of power grid resilience, although it possesses several drawbacks. The precision of the proposed framework is significantly contingent upon the quality of input data, especially fragility curves and seismic hazard models. In areas with insufficient seismic data, the dependability of these inputs may be undermined, impacting the overall efficacy of the resilience methods. One solution to such constraint may refer to partnering with scientists, scholars and applying modern technologies such as satellite surveillance and IoT-integrated devices to obtain more accurate results.

This study mainly emphasizes technical issues, including load islanding and load flow analysis, but socio-economic and logistical factors are not thoroughly explored. The viability of implementing protective load islanding in densely populated urban areas or resource-constrained locations requires further research. Integrating stakeholder viewpoints and performing multidisciplinary research may yield a more comprehensive understanding of resilience planning. Currently proposed methodology assumes and presents a centralized decision-making process for the implementation of resilience measures, which may not necessarily correspond with decentralized energy systems or regulatory frameworks in specific regions. Future study may investigate decentralized methodologies for resilience planning, integrating local community participation and the management of distributed energy resources.

CHAPTER TWO

REVIEW OF LITERATURE

There has been observed an drastic increase in the number of studies on improving the resilience of power grids to high-impact, low-probability (HILP) events [3], focusing on hardening power grid, mitigation strategies and adaptive operational measures. Many of them explore the utilization of theoretical methods such as seismic hazard characterization, risk assessments, algorithmic procedures and advanced resilience solutions such as protective isolation and real-time monitoring systems. This literature review adopts a structured approach, starting with an overview of seismic risks to power systems, followed by analysis of power grid vulnerability to natural hazards, enhancement of reselience and long term mitigation strategies. Finally, it identifies research gaps and challenges, setting the stage for the proposed methodology.

A. Hazard Characterization

In the discipline of earthquake modeling for power grid resilience, hazard characterization employs a diverse array of methodologies to comprehensively assess seismic risks and enhance the resilience of critical infrastructure. Central to this effort are several key methodologies and simulation techniques that were deployed in most of the papers:

- *Seismic Hazard Assessment (SHA)*

  This foundational method evaluates the probability of various levels of ground shaking occurring at specific sites over a defined period. Probabilistic Seismic Hazard Analysis (PSHA) encompasses uncertainties in earthquake parameters such as location, magnitude, and ground motion prediction equations based on site-specific parameters such as soil type, for instance, to quantify seismic hazard probabilities. On the contrary, Deterministic Seismic Hazard Analysis (DSHA), is centralized on estimating ground shaking from specific earthquake scenarios, most of the times considering worst-case scenarios for fault movements [12], [41].

- *Ground Motion Characterization*

  Attenuation ratios (AR) [3], also known as ground motion prediction equations (GMPE), play a critical role in characterizing how seismic intensity decreases with distance from an earthquake source. These ratios incorporate factors such as earthquake magnitude, distance, and local soil conditions to predict peak ground acceleration (PGA), peak ground velocity (PGV), and spectral acceleration (SA). Such metrics provide a detailed understanding of how different structures and components in power systems will respond to varying levels of ground shaking [40].

- *Monte Carlo Simulation (MCS)*

  MCS is used to generate a wide range of earthquake scenarios by considering the stochastic nature of ground motion.[3] Using random sampling and statistical modeling, MCS generates numerous seismic events that capture the variability and uncertainties inherent in earthquake phenomena. It can generate up to thousands of earthquake scenarios within short duration of time. Finite element modeling (FEM) is another important tool that simulates the dynamic response of infrastructure components to ground shaking, allowing for detailed analysis of potential damage mechanisms and structural vulnerabilities [40].

- *Fragility Curves (FCs)*

  Fragility curves (FCs) are broadly used graphically depicted tools in seismic vulnerability assessments with the probability of different damage states (slight, moderate, extensive, complete) as a function of seismic intensity measures like Peak Ground Acceleration (PGA) or spectral acceleration (SA). According to the HAZUS [8], these damage states are defined by specific parameters in the table below:

Damage State	Occurrence
Slight	5% fail
Moderate	40% malfunction
Extensive	70% fail
Complete	100% system fail

Table 1. Damage States

These thresholds provide a structured basis for effectively assessing and mitigating potential seismic damage to substations. Fragility curves, whether derived from empirical data, analytical models or expert judgement, provide critical insight into the performance and resilience of electricity generation facilities, transmission lines and substations under earthquake conditions. Figure 1 [8] depicts a fragility curve that plots the relationship between earthquake intensity (x-axis) and the probability of structural damage (y-axis), illustrating how the probability of damage increases with seismic intensity.

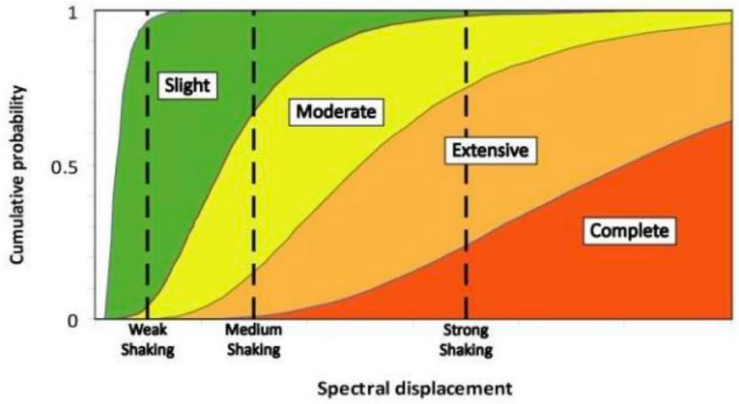

Figure 2. Fragility Curves [8]

- *Geospatial Analysis*

  Geographic Information Systems (GIS) are being utilized by most of the geoscientists in spatially mapping and analyzing seismic hazards, including fault lines, historical earthquake occurrences, and soil properties.[56],[57].

- *Fault Tree Analysis (FTA)*

  FTA is used to systematically assess the vulnerability of power plant components by identifying potential failure modes and their probabilities. By breaking down complex systems into logical event-condition diagrams, FTA helps to prioritize mitigation measures such as structural strengthening, component anchoring, and soil stabilization techniques to effectively mitigate seismic risks [51],[52],[54].

In combination, these methodologies enable a comprehensive hazard characterization approach that is essential for developing resilient strategies to safeguard power grids against seismic events. By integrating advanced modeling techniques, empirical data, and geospatial analyses, researchers and engineers can effectively assess, mitigate, and manage the impacts of earthquakes on critical infrastructure, ensuring the continuity of electricity supply and minimizing societal and economic disruptions.

B. Power Grid Vulnerability to Earthquakes

Power Grid Vulnerability encompasses three key elements of today's power grid: power generation, power transmission, substations, and distribution systems. These components are interdependent of each other and susceptable to various risks, including the earthquakes.

Power Generation System

While most of the recent studies on resilience are concentrated on substation level, there are few studies on generating frameworks/models for monitoring seismic effects on power generation plants. A feasible earthquake disaster model is built and the framework for resilience & risk

assessment of electric-gas system under earthquake is proposed in [10]. In [53] authors proposed an automated system for seism metric monitoring in hydroelectric power plants.

Power Transmission System

Power transmission lines are highly vulnerable to earthquakes due to potential ground shaking and displacement, which can cause structural damage and disruptions in electricity transmission. Seismic events can severely impact power transmission lines by causing structural damage and connection loss. One study proposes a methodology to evaluate these impacts, focusing on pipeline leakage and transmission line failures using a stochastic model. By classifying seismic impacts according to damage levels and quantifying load curtailment, the study demonstrates how earthquakes can overload transmission lines and limit generation capacity, emphasizing the need for resilience enhancement schemes based on the vulnerability of integrated energy systems. Furthermore, a comprehensive study on gas-insulated transmission lines (GIL) in ultra-high-voltage converter power plants reveals their seismic weak points and failure modes, such as housing strength failure and displacement-exceeding-limit failure. [13] By analyzing dynamic amplification effects and testing retrofit methods, the study demonstrates that fixing connections between sliding supports, and the housing significantly reduces GIL seismic vulnerability by over 50%. [13]

Power Substation and Distribution Systems

Power substations and distribution systems are vital components of electrical infrastructure posed to seismic events, particularly due to the structural integrity challenges caused by earthquakes. Recent catastrophic events, such as the 2008 Wenchuan earthquake in China and the 2011 Tohoku earthquake in Japan, have underscored the severe impact on power transformers and their bushings, resulting in widespread disruptions and substantial economic losses [36]. These incidents underscore the immediate need for enhancing the seismic resilience of substations through detailed vulnerability assessments and mitigation strategies. Studies have identified that transformers and their components, such as bushings, are particularly prone to damage, often leading to prolonged outages and significant repair costs. Research has utilized advanced techniques such as Finite Element Modeling [46], and seismic vulnerability assessments to evaluate the performance of transformers under seismic loads. Strategies like retrofitting vulnerable components and employing base isolation techniques have been proposed to mitigate seismic risks effectively. Moreover, efforts to develop fragility functions and probabilistic models for substations aim to provide decision-makers with crucial insights into vulnerability, aiding in the development of resilience enhancement measures.[43]

C. Resilience Enhancing Solutions

In order to enhance power grid resilience, numerous researchers have been concentrating on using modern tactics and technologies, with a particular emphasis on sophisticated restoration techniques, operational measures, early warning systems, and structural hardening. Together, these strategies address the intricate problems posed by seismic hazards, providing a strong basis for the development of robust and flexible power systems.

Power Grid Hardening

Methods for improving power grid resilience can be roughly divided into two categories: operational and hardening measures. The goal of hardening measures is to make infrastructure more physically resilient to calamities like earthquakes. Retrofitting substations with robust parts like composite insulators and anchored transformers, strengthening distribution poles and modernising transmission towers are a few examples [6]. These initiatives seek to minimise downtime and physical damage, which are crucial during seismic occurrences when substations are most susceptible [6]. On the other hand, operational strategies, such as island microgrid operation and defensive islanding, concentrate on flexible reactions to keep the grid running even in the face of interruptions [6]. These steps include using distributed energy resources (DERs) such as gas turbines to supply key loads during emergencies and implementing sophisticated load restoration strategies [6]. Operational strategies improve responsiveness and flexibility in handling grid outages brought on by earthquakes and other extreme events. Deterministic and probabilistic earthquake models are important for assessing the seismic resilience of power systems. While probabilistic models evaluate many possible earthquake scenarios to better prepare for varying degrees of damage, deterministic models consider worst-case scenarios based on maximum magnitude and proximity to faults [7]. When constructing resilient power grids that can successfully endure and recover from seismic events, both kinds of models are used to inform decision-making. These integrated strategies emphasize how crucial it is to combine operational and hardening measures to improve power system resilience overall. By adaptive operational techniques and the concomitant reinforcement of physical infrastructure, utilities and policymakers can mitigate risks, reduce vulnerabilities, and ensure reliable electricity supply in the face of seismic challenges.

Earthquake Early Warning Systems (EEWS)

Earthquake early warning systems (EEWS) are key tools designed to provide advance notice of upcoming seismic events, which is critical to mitigating potential damage and saving lives. Authors discussed in [17], [18], [20], [21] that EEWS use a network of distributed seismometers to detect the initial P-waves, which travel faster than the consecutive, more destructive S-waves of an earthquake. By quickly analyzing ground motion data, EEWS can issue targeted alerts to regions likely to experience significant shaking, thereby allowing timely protective measures to be taken. Recent advancements in deploying this strategy include the development of low-cost seismic prototypes using technologies such as Arduino IOT microcontrollers and ADXL345 accelerometers, which can provide on-site earthquake early warning notifications within seconds of seismic wave detection [18], [23]. Furthermore, the integration of deep learning techniques such as convolutional neural networks (CNNs) and long short-term memory (LSTMs) has improved the accuracy of seismic event detection in various seismometer networks, as demonstrated by studies using large seismic signal datasets [15], [26]. IoT-based solutions using MEMS technology have demonstrated the ability to detect events with a magnitude of over 4.1 and alert within a radius of 30 km, further supported by IoT cloud architectures for real-time event monitoring and alarm signal dissemination [19], [24], [25]. These achievements underscore the important role of EEWS in improving disaster preparedness and response, facilitating proactive measures aimed at enhancing community resilience to earthquakes and other natural disasters.

D. Mitigation Strategies for Power System Resilience

Increasing the energy system's resistance to seismic activity necessitates a multipronged strategy that incorporates operational tactics and structural reinforcement. Microgrids, which serve as local physical islands with the ability to use distributed energy resources (DER) to provide a continuous power supply in an emergency, are one of the main alternatives [38]. Although microgrids provide local resilience, they are not very good at supporting loads that are located farther away. In order to tackle this problem, mobile energy sources (MES) like electric vehicles (EV), mobile emergency generators (MEG), and mobile energy storage systems on truck chassis (MESS) offer more flexibility and support because of their mobility, which enables quick deployment in crucial locations [38].

Research emphasises how crucial planning and routing are for electric vehicles (EVs) and multi-disciplinary energy groups (MEGs) to enhance the distribution system's (DS) resilience, enabling dynamic resource distribution and speeding up recovery [34]. Additionally, by rerouting the energy supply to vital loads and improving system resilience, remotely controlled switches (RCS) enable the reconfiguration of the distribution system (DS) network. following the quake [38].

earthquake reinforcing plans are essential for enhancing substations' earthquake resilience. The reliability of substations during earthquakes is greatly increased by these measures, which include but are not limited to strengthening disconnectors and increasing the number of transmission lines aimed at key consumers [9]. Furthermore, as evidenced by the plans for allocating emergency repair teams for the successive restoration of transmission lines and renewable energy facilities, the integration of energy and transportation systems enhances emergency response and guarantees successful system recovery and reintegration following an earthquake [11]. Solutions for disaster response without emissions are provided by the deployment of photovoltaic (PV) systems, particularly microgrid PVs and sustainable solar energy concepts for communities [30]. The efficiency of mitigation techniques for power lines during catastrophes is further improved by strengthening construction and energy standards, evaluating the quality of the power supply, and evaluating the results of emergency response [34]. These all-encompassing methods highlight how crucial it is to combine dynamic operational techniques with structural strengthening in order to increase the energy system's overall resilience to seismic risks.

E. Grid Restoration Strategies

Efficient restoration and recovery strategies are crucial for enhancing the resilience of power distribution networks (PDNs) in the chain reaction of seismic events. One innovative approach involves leveraging Vehicle-to-Grid (V2G) technology to expedite power supply recovery. In this strategy, an economic recovery model integrates distribution network reconfiguration with V2G reverse transmission [28], considering the autonomous behavior of electric vehicle (EV) users through pre-disaster strategies and post-disaster response mechanisms in [28]. This method optimizes the utilization of EV batteries as mobile energy storage units, aiding in restoring critical loads smoothly and efficiently. Additionally, methodologies like the simulated annealing (SA) algorithm optimize scheduling by considering geographical routes and the multi-state nature of infrastructure, thereby improving the efficiency of PDN restoration post-earthquake [29]. By simulating various scenarios and utilizing optimization algorithms, these approaches ensure that

resources are allocated optimally to minimize downtime and expedite recovery efforts. Furthermore, to minimize total functionality loss following seismic occurrences, a resilience-based recovery method optimizes electrical substation equipment repair sequences using heuristic algorithms within a systemic evaluation framework [35]. This strategy involves establishing a direct relationship between the seismic resilience index of substation systems and the sequence of equipment repairs, employing genetic algorithms to identify the most optimal repair sequence under limited emergency resources and initial damage conditions.

The strategies highlight the importance of integrating advanced optimization techniques and innovative technologies to enhance the resilience and operational continuity of power systems following natural disasters, thereby ensuring reliable electricity supply during critical periods of recovery.

CHAPTER THREE

RESEARCH METHODOLOGY

Figure 3 presents the basic framework for implementing grid resilience enhancement using defensive islanding technique. This framework focuses on identifying seismic hazard modeling and fragility curves, performing load flow analysis, and implementing protection island using spectral clustering, the details of which are provided in this chapter. The IEEE 24-bus system functions as an experimental framework for evaluating the methodology. The combination of MATLAB and the MATPOWER library provides a computational framework for implementing the proposed methods. The main objective is to minimize the probability of cascading failures during seismic events, improve post-event recovery, and provide actionable insights into the effectiveness of advanced resilience strategies for power grids.

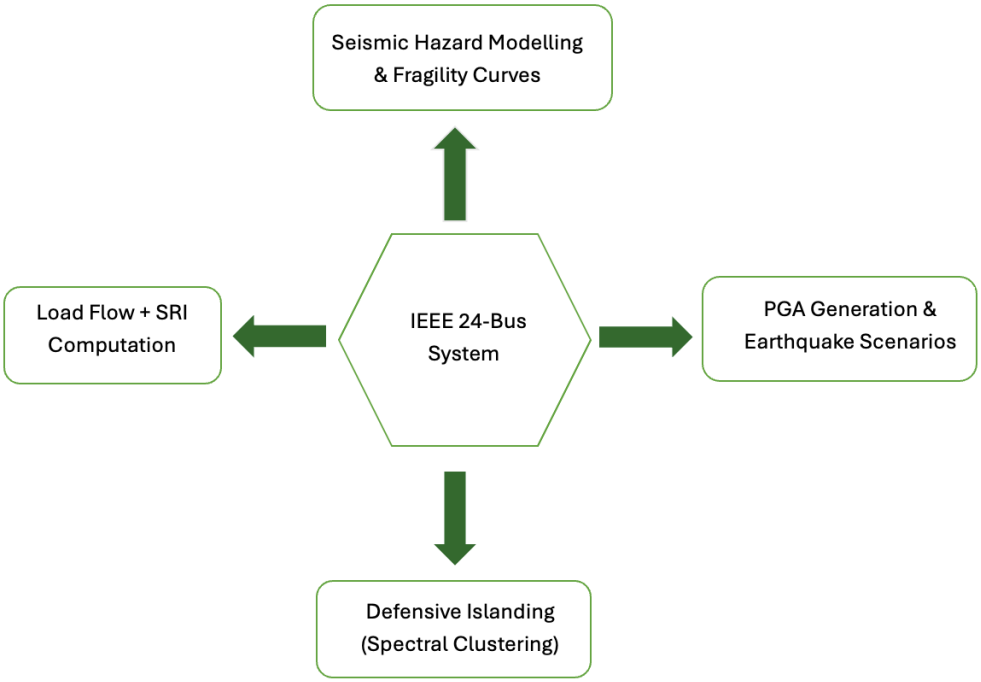

Figure 3. Main Framework Structure

Seismic Hazard Modelling

Seismic hazard modeling is essential for assessing seismic risks, concentrating on the propagation, attenuation, and effects of seismic waves on infrastructure. This approach integrates physical principles, mathematical modeling, and probabilistic techniques to evaluate potential ground motion at key sites within the power grid. The outputs from hazard modeling, specifically the Peak Ground Acceleration (PGA), are critical inputs for the development of fragility curves and resilience analysis.

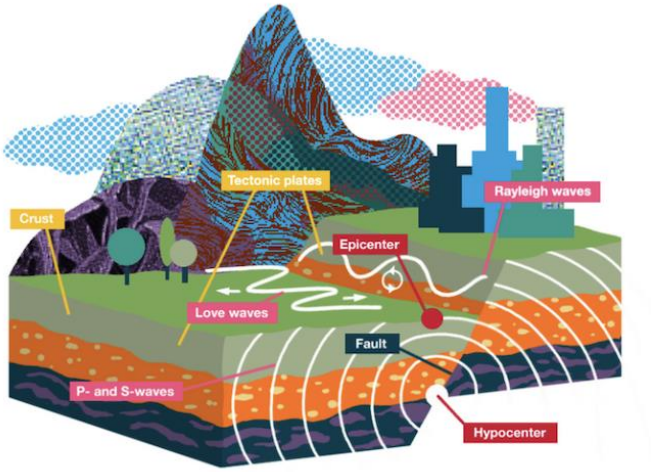

Figure 4. Illustration of Seismic Wave Propagation and Earthquake Dynamics

Seismic waves produced by an earthquake are classified into primary (P) waves, secondary (S) waves, and surface waves which include Rayleigh Waves and Love Waves. P waves, characterized by their compressional nature, propagate most rapidly through solids, liquids, and gases. Although they arrive first, their reduced amplitude generally leads to limited structural damage. S waves, which succeed P waves, exhibit slower propagation yet possess greater destructiveness attributable to their larger amplitude. The waves generate horizontal and vertical motion, potentially compromising the integrity of infrastructure. Surface waves propagate along the Earth's surface and, while they arrive last, they inflict the most significant damage near the epicenter due to their elevated amplitude and extended duration of shaking.

An earthquake's location is characterized by the hypocenter, which is the point beneath the Earth's surface where the rupture begins, and the epicenter, which is the point on the surface directly above the hypocenter. Seismic waves propagate outward from the hypocenter, resulting in a decrease in ground motion intensity due to attenuation. The attenuation is affected by the distance from the source, geological properties of the medium, and local topographical features. Soft soils amplify seismic waves, resulting in increased peak ground acceleration (PGA), while rocky terrain typically attenuates seismic motion.

The study utulizes an attenuation relationship (AR) to quantify this attenuation. The AR is a mathematical model that connects earthquake parameters, including magnitude, distance, and site conditions, to the intensity of ground motion. According to [59] the standard representation of the AR is as follows:

$$\ln(\Psi) = \nu + f_1(M) + f_2(R) + f_3(Z) + \varepsilon \quad [59]$$

where:

- Ψ : A parameter representing ground motion, such as Peak Ground Acceleration (PGA).
- M : Magnitude of an earthquake (e.g., measured on the moment magnitude scale).
- R : Distance from the seismic source, either epicentral or hypocentral.
- Z : Characteristics specific to the site, including soil type, sediment thickness, and topography.
- ν : A constant variable.
- $f_1(M)$: A function that characterizes the influence of magnitude on ground motion.
- $f_2(R)$: A function that characterizes the attenuation effect as a function of distance.
- $f_3(Z)$: A function that denotes site amplification effects.
- ε : A random error term that signifies the uncertainty inherent in the model.

The functions f1(M), f2(R), and f3(Z) are derived empirically from historical seismic data using statistical regression methods. For example, f2(R) may include terms such as $\alpha \cdot \ln(R)$, where α serves as a coefficient that indicates the attenuation rate.

Due to the stochastic characteristics of seismic events, the study uses Monte Carlo simulation (MCS) to generate probabilistic earthquake scenarios. This entails sampling earthquake magnitudes, distances, and on-site conditions informed by regional seismicity and geological data. In each scenario, AR calculates PGA values at specific locations within the power grid, including substations, busbars, and transmission lines.

The computed PGA values offer a spatially explicit depiction of seismic hazards. Earthquake modeling identifies components of the power system that are most susceptible to high-intensity ground motion by mapping relevant values to these components. This spatial mapping incorporates local geological and topographical features, ensuring that the model accurately represents the site-specific characteristics of the power grid. Figure 4 visually summarizes the physical principles underlying hazard modeling, illustrating the propagation of seismic waves from the hypocenter and their attenuation with distance. The figure illustrates the impact of local site conditions, including soil type, on the amplification of seismic waves, resulting in elevated PGA values in specific regions. This conceptual framework is implemented in the augmented reality and probabilistic simulations, establishing a direct link between the physical behavior of seismic waves and their mathematical representation.

Earthquake modeling offers a comprehensive framework for evaluating the potential effects of earthquakes on power grids. The integration of seismic wave propagation physics, mathematical modeling through AR, and probabilistic simulation via MCS produces realistic and actionable inputs for the development of fragility curves. This integration captures both the physical and probabilistic aspects of seismic events, establishing a foundation for thorough vulnerability analysis and resilience planning.

A. Identification of Fragility Curves

The framework provides a probabilistic approach to assessing the likelihood that infrastructure will reach or exceed specified damage states in response to varying levels of ground motion, including peak ground acceleration (PGA). Fragility curves act as a link between hazard characterization and system-level resilience analysis, facilitating informed decision making for mitigation and restoration strategies in this study. This section describes the development, calibration, and application of fragility curves for assessing seismic vulnerability of power systems. The importance of fragility curves in improving seismic resilience is of paramount importance.
Fragility curves estimate the probability of damage to a component or system with respect to a measure of seismic intensity, typically represented by PGA. Probabilistic representation of damage states provides insight into the vulnerability of individual components, including transmission lines, substations, and transformers, as well as the entire power grid. Fragility curves are important because of their ability to:

- Incorporate Uncertainty: Seismic events have inherent unpredictability, characterized by variability in magnitude, distance, and local soil conditions. Fragility curves incorporate these uncertainties by linking damage probabilities to different levels of seismic intensity.
- Support Resilience Strategies: Fragility curves facilitate the identification of the most vulnerable components, thereby informing the allocation of resources for strengthening and operational strategies.
- Enable System-Level Analysis: The integration of fragility curves with network-level simulations offers a detailed understanding of potential cascading failures and associated recovery requirements.

B. Damage States

Fragility curves generally span through various damage states, from none to total damage. The states are delineated according to structural, mechanical, or operational criteria pertinent to the component under analysis. In power systems, potential damage states are following:

Type of Damage States	Probability of Each State	Post-quake Accessibility
No Damage	$P_N = 1 - P[Sl\|\rho]$	100
Slight Damage	$P_{Sl} = P[Sl\|\rho] - P[M\|\rho]$	100
Moderate Damage	$P_M = P[M\|\rho] - P[E\|\rho]$	50
Extensive Damage	$P_E = P[E\|\rho] - P[C\|\rho]$	0
Complete Damage	$P_C = P(C\|\rho)$	0

Table 2. Classification of Damage States, Probabilities and Accessibility Levels [3]

Table 2 demonstrates the response of power generation units and other essential infrastructure to seismic events, highlighting the differing probabilities of damage states and their effects on post-earthquake accessibility. A well-reinforced generation facility may sustain minimal damage during moderate seismic activity, preserving full functionality, while less resilient units may incur moderate to extensive damage, resulting in reduced or complete operational loss. Each damage

state is associated with a probability that is contingent upon the seismic intensity parameter. The probabilities indicate the likelihood of a unit transitioning into each state. Post-earthquake accessibility differs based on damage levels: full functionality is maintained for no or slight damage, partial operation is possible at 50% capacity for moderate damage, and total inaccessibility occurs with extensive or complete damage. Taking into coniderations various variables affecting the grid such as location and proximity to earthquake epicenter, diffferent responses are generated after an HILP event.

C. Methods for Analysing & Implementing Fragility Curves

Fragility curves are obtained using one or more of the following methods:

- Empirical Method: Historical observations of earthquakes offering concrete evidence regarding the performance of components subjected to seismic stress. However, the data may have certain limitations or inconsistencies.

- Analytical Method: Structural and mechanical models that reproduce the behavior of components under varying seismic intensities. These models use finite element methods, dynamic analysis, or alternative computational methods to estimate the probability of damage.

- Expert Judgment: Expert opinions that offer estimates regarding component vulnerability based off practical experience.

- Hybrid Method: By using both analytical and experimental methods, obtaining fragility curves

The mathematical formulation is an essential component of problem-solving across multiple disciplines. It entails converting real-world situations into mathematical expressions and equations, facilitating systematic analysis and solution derivation. The correlation between peak ground acceleration (PGA) and the likelihood of damage states is generally depicted by a lognormal cumulative distribution function (CDF).

$$P[\vartheta|S_d] = \Phi\left[\frac{1}{\sigma_\vartheta} ln\left(\frac{S_d}{\overline{S}_{d,\vartheta}}\right)\right] \quad [3]$$

where:

- P : probability of achieving or surpassing a specified damage state.
- S_d : the spectral displacement.
- $S_{d,\theta}$: median value
- σ_θ : the standard deviation
- Φ : the standard cumulative normal distribution function.

Fragility curves, once developed, are utilized to assess the seismic vulnerability of power grid components. The integration of fragility curves with Monte Carlo Simulation (MCS) and load flow analysis is used to evaluate system-wide impacts. The PGA values produced via MCS are utilized in fragility curves to determine the damage probabilities for each component. To assess the electrical grid's overall resilience, damage probability are combined. This entails determining crucial elements whose malfunction could cause a chain reaction of outages. Lastly, the results help prioritize hardening measures, operating plans, and the distribution of resources for post-earthquake recovery.

Load Flow Analysis

In power system studies, load flow analysis is crucial for evaluating the electrical grid's steady state operation. It offers vital information about system losses, active and reactive power flows, phase angles, and busbar voltages. Power grid planning, operation, and optimization all depend on this analysis. The Newton-Raphson approach [61] is employed in this study to analyze load flow, emphasizing its superior convergence characteristics and capacity to manage large, complicated systems with nonlinear variable interactions.

A. Methods for Load Flow Analysis

Resolving a system of non-linear equations that describe the relationships between power injections, voltage magnitudes, and phase angles at different buses is the task of load flow issues. Numerous numerical techniques have been developed to solve these equations, such as:

- Gauss-Seidel Method: an iterative approach which updates the bus voltages sequentially until convergence is achieved. This method is computationally efficient and requires minimal memory, making it suitable for small power systems. However, its convergence is highly dependent on the initial assumption and shows poor performance in large networks or systems characterized by ill-conditioning. Therefore, Gauss-Seidel Method can be considered as impractical for modern large-scale networks due to its inefficiency.

- Fast Decoupled Load Flow Method: categorizes active and reactive power calculations, relying on the premise of weak interdependence between voltage magnitude and phase angle, and then displays results in the form of power flow equations. It demonstrates computational efficiency and low memory usage, meaning that it is practical for real-time applications. However, such reliance may result in inaccuracies, especially in systems characterized by high resistance-to-reactance (R/X) ratios or under heavily loaded conditions.

- Newton-Raphson Method: an iterative technique to linearize power flow equations through Taylor series expansion. It demonstrates quadratic convergence, indicating that the error decreases exponentially with each iteration, thus enhancing its efficiency for addressing large-scale systems. This method demonstrates robustness across diverse operating conditions and is independent of simplifying assumptions, thereby ensuring high accuracy.

The Newton-Raphson method was chosen for this study because of its computational efficiency, precision, but mostly due to its ability to manage complex, interconnected grids. The procedure for implementing this method consists of the following steps:

1. Formulation of Power Discrepancies:
   The mismatches in active and reactive power (ΔP_i and ΔQ_i) are as follows:

$$\Delta P_i = P_i^{specified} - P_i^{calculated} \quad [61]$$

$$\Delta Q_i = Q_i^{specified} - Q_i^{calculated} \quad [61]$$

   The identified discrepancies are utilized for the determination of necessary adjustments in bus voltages and phase angles.

2. Linearization of Equations and the Jacobian Matrix:

   Power mismatches are represented through voltage magnitude ($|V|$) and phase angle (δ) corrections, utilizing the Jacobian matrix (J):

$$[\Delta P] = [H\ N]\ [\Delta\delta] \quad [61]$$
$$[\Delta Q] = [M\ L]\ [\Delta|V|] \quad [61]$$

   where:
   - (H, N, M, L): Submatrices of the Jacobian, obtained from the partial derivatives of (P) and (Q) concerning (δ) and ($|V|$)
   - ΔP and ΔQ: Represent power mismatches
   - ($\Delta\delta$) and ($\Delta|V|$): Adjustments to voltage phase angles and magnitudes.

3. Resolution of Linearized Equations:
   The corrections are determined by solving the linearized equations.

$$[\Delta\delta] = [\Delta P] \quad [61]$$
$$[\Delta|V|] = [\Delta Q] * J^{-1} \quad [61]$$

4. Voltage Updates: The bus voltages and phase angles are updated as follows:

$$\delta_i^{(k+1)} = \delta_i^{(k)} + \Delta\delta_i, \quad [61]$$
$$|V_i|^{(k+1)} = |V_i|^{(k)} + \Delta|V_i| \quad [61]$$

   here k is the number of iterations through which the voltages and phase angles are being updated, i refers to arbitrary number of the bus.

5. Convergence Check: Iterations proceed until the discrepancies ΔP and ΔQ fall below a specified threshold (ϵ), commonly set at 10^{-6}.

B. Implementation of the Newton-Raphson Method

This study employs the Newton-Raphson method utilizing MATLAB. The subsequent steps delineate the implementation process:

- Initialization: The magnitudes and phase angles of the bus voltage are going to be initialized. The slack bus voltage is maintained at a fixed value ($|V_1| = 1.0$ per unit and $\delta = 0$ degrees), with flat-start values applied to the remaining buses.

- Formulation of the Y-Bus Matrix: The admittance matrix (Y_{ik}) is derived from the network data, which includes line impedances and shunt admittances.

- Iterative Solution: The Jacobian matrix undergoes updates, and adjustments to voltages and angles are implemented in each iteration until convergence is reached.

- Output Results: The final solution is going to encompass voltage magnitudes and phase angles at all buses; power flow analysis for both active and reactive components on each line; overall system losses.

The Newton-Raphson method is particularly suitable for this study due to its quadratic convergence, which improves efficiency in large systems. It solves nonlinearities in the power flow equations without the need for simplifications. It demonstrates stability under a variety of operating conditions, covering both heavily loaded and loosely interconnected networks. It provides accurate results, ensuring reliability in the analysis of complex power networks. This method facilitates accurate and reliable load flow analysis, serving as a basis for subsequent stability assessments and optimization studies under seismic conditions.

Defensive Islanding Using Spectral Clustering

This section outlines the methods for executing defensive islanding via spectral clustering to enhance the durability of the IEEE 24-bus system under seismic conditions.

A. Representation of the Power Grid as a Graph

The power grid is represented as a weighted graph G(V, E, W), where:

- V denotes the set of nodes, which correspond to buses in the grid.
- E denotes the set of edges, which represent transmission lines connecting buses.
- W represents the weighted adjacency matrix, which encodes the strength of connections among nodes.

The weights in the adjacency matrix are obtained from the power flow between buses. For a line connecting buses i and j, the weight w_{ij} is defined as follows:

$$w_{ij}=(|S_{ij}|+|S_{ji}|)/2 \qquad [60]$$

where S_{ij} refers to the apparent power flow from bus i to bus j , and S_{ji} denotes the flow in the opposite direction. This representation ensures that the graph accurately reflects the operational interdependencies present in the grid.

B. Spectral Clustering

As it was mentioned in previous sections, spectral clustering sections the power grid into smaller, self-sufficient islands. It uses the graph Laplacian matrix (L) which is defined in relation to the adjacency matrix (W) by the equation:

$$L = D - W \qquad [60]$$

where D represents the degree matrix, a diagonal matrix characterized by the entries $D_{ii}=\sum_j w_{ij}$.

The normalized spectral clustering Laplacian is defined as:

$$L_n = I - D^{-1/2} W D^{-1/2} \quad [60]$$

where I represents the identity matrix.

The eigenvalues and eigenvectors of the Laplacian matrix represent the connectivity structure of the graph. The smallest k eigenvalues and their associated eigenvectors are utilized to partition the nodes into k clusters. Each group functions as a distinct entity.

C. Incorporation of Seismic Vulnerabilities

The methodology for adapting spectral clustering to seismic resilience incorporates data on component vulnerabilities. Fragility curves estimate the probability of damage to each bus and line based on the Peak Ground Acceleration (PGA) experienced during an earthquake. Buses and lines exhibiting elevated failure probabilities are designated as critical.

A constraint matrix C is established to ensure that vulnerable components are clustered within the same island. The constrained Laplacian is expressed as:

$$C^T L_n C u = \lambda C^T C u, \quad [60]$$

where u represents the eigenvector associated with the smallest eigenvalues. This formulation isolates vulnerable components, thereby minimizing their impact on the remainder of the grid.

D. Optimization of Load-Generation Balance

Following the formation of the islands, an assessment of their operational feasibility is conducted. Each island must attain equilibrium between load and generation.

$$P_k^{generation} = P_k^{load} + P_k^{loss} \quad [60]$$

where :

- $P_k^{generation}$ refers to the total power generation in island k
- P_k^{load} refers to the total load in the island
- P_k^{loss} refers to the transmission losses

In the absence of balance, load shedding is implemented according to established priorities, including critical infrastructure and consumer categories.

E. Voltage and Frequency Stability Constraints

To maintain stable operation, each island must adhere to the following constraints:

- Voltage Stability:

$$V_{min} \leq V_i \leq V_{max}, \forall_i \in \text{Island k}, \quad [60]$$

where V_{min} and V_{max} represent the permissible voltage limits.

- Frequency Stability:

$$|f_k - f_0| \leq \Delta f_{max}, \forall k, \quad [60]$$

where f_0 represents the nominal frequency, and Δf_{max} denotes the maximum permissible deviation.

F. *Severity Risk Index (SRI)*

The Severity Risk Index (SRI) is a critical metric for assessing the risk of potential power system breakdowns resulting from seismic events. It serves as a decision-making instrument for beginning protective islanding by evaluating the likelihood and ramifications of cascading failures. The SRI integrates seismic hazard statistics, component vulnerabilities, and system-wide operational impacts to deliver a comprehensive evaluation of the grid's resilience during earthquakes.The SRI integrates the failure probability of essential components with the potential consequences of those failures on the power system. Mathematical representation of such metric is as followed:

$$SRI=\sum_{k=1}^{K} P_k * I_k \quad [60]$$

where:

- P_k: Probability of failure for scenario k, obtained using seismic hazard models and fragility curves.

- I_k: The effect of failure scenario k, measured through system performance measures such load shedding, voltage fluctuations, or cascading failures.
- K: The aggregate number of earthquake situations evaluated.

The SRI functions as a catalyst for commencing defensive islanding. When the SRI above a specified level, it signifies a significant probability of cascading failures and warrants the implementation of defensive islanding methods. The procedure is as followed:

First, seismic monitoring systems and grid sensors deliver instantaneous data regarding ground motion, electricity flows, and component status. The SRI is calculated continuously using the most recent data. High-risk components are identified, and their failure probabilities are adjusted in real-time. Then, Spectral clustering is utilized to segment the grid into islands, thereby isolating susceptible components and mitigating the consequences of their failure.
At the final stage, the efficacy of islanding is evaluated by re-computing the SRI for the detached grid. A substantial decrease in the SRI signifies effective risk minimization.

G. *Defensive Islanding Algorithm*

Figure 5 generated by [60] represent the overall defensive islanding algorithm which is implemented by incorporating the rest methodologies and metrics mentioned in this paper. The flowchart demonstrates a sequential representation of the defensive islanding process, illustrating the algorithm's response to extreme events, risk assessment, and implementation of operational solutions to maintain grid stability. Every stage in the flowchart represents an essential component of the decision-making and resilience-building process.
The system advances iteratively, incorporating real-time monitoring data to reassess risks and adjust conditions. The execution process continues until the event's effects are fully addressed, the grid is stabilized, or no further dangers are identified. Such algorithm enhances the grid's resilience by adaptively responding to fluctuating conditions, ensuring that essential operations continue despite poor circumstances.

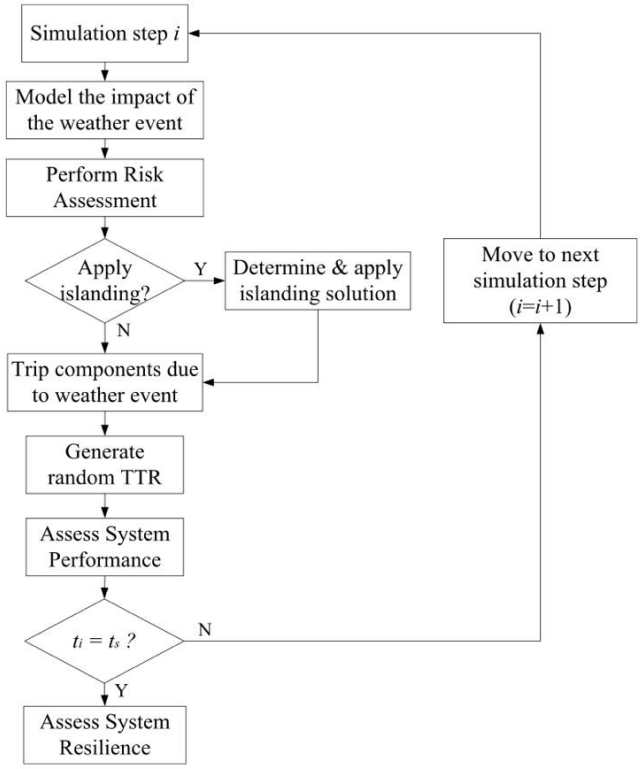

Figure 5. Defensive Islanding Algorithm [60]

CHAPTER FOUR

RESEARCH ANALYSIS AND RESULTS

A. Case Study: IEEE 24-Bus Test System

1. Description of The Test System:

The IEEE 24-bus test system is a common way to check the performance, dependability, and resilience of the power grid. It is made up of 24 buses, which stand for power network points or substations. Transmission lines connect these buses, making a network that makes it easier for power to move between generators and loads.

Ten generation units are spread out across several cars in the system. Size-wise, these units range from 100 MW (on Bus 7) to 400 MW (on Bus 18 and Bus 21), with the bigger engines being able to provide that much power. Some buses, like Bus 23, have more than one engine to make sure they are reliable and can meet local demand. The network has a spread of loads,

with bigger concentrations at some buses, like Bus 13, which can handle a lot of traffic. To keep the system balanced, smaller loads are spread out among other buses, such as Buses 1, 2, and 3.

The transmission network uses lines and transformers to connect the buses. This makes it easy for power to move from places where it is made to places where it is needed. Real-world features like impedance and temperature limits are modeled by these lines. This lets us do more in-depth studies of grid stability and power flow.

The system also has substations that control the flow of power and how buses link to each other. These links offer backup and help keep the grid stable when something goes wrong. Please see the picture below of a Single Line Diagram for our type. A lot of people use this test case to look at load flow, try defensive islanding strategies, see how well systems work when there are problems, and find ways to make the grid more resistant to outside events like earthquakes. Further simulations are implemented using MATLAB and MATPOWER library.

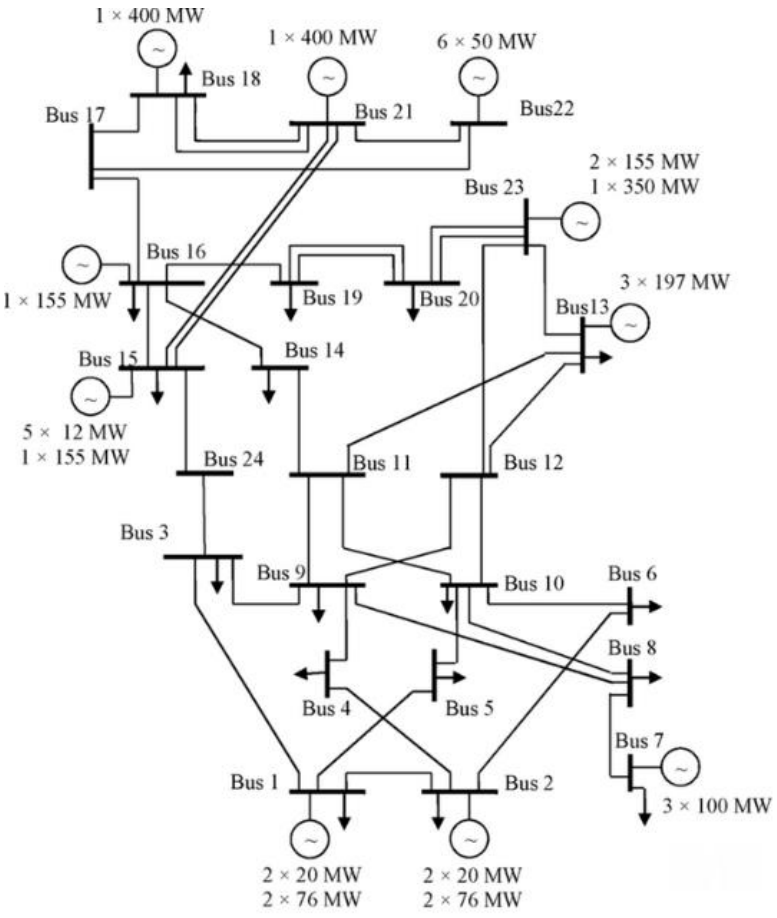

Figure 6. IEEE 24-Bus Single Line Diagram

2. Load Flow Analysis

The load flow analysis results for the IEEE 24-bus system offer a comprehensive insight into the system's steady-state operational circumstances. The analysis relies on the MATPOWER power flow outcomes. Figure 7 illustrates the summary of the load flow analysis. The convergence of the Newton-Raphson method within merely 4 iterations in 0.20s illustrates the numerical stability and robustness of the system model.
The subsequent parts analyze the system overview, bus data, generator outputs, and branch flows comprehensively, providing insights into system performance and operational stability.

```
Newton's method converged in 4 iterations.
PF successful

Converged in 0.20 seconds
================================================================================
|     System Summary                                                           |
================================================================================

How many?                How much?              P (MW)            Q (MVAr)
---------------------    -------------------  -------------  -----------------
Buses              24     Total Gen Capacity    3405.0         -535.0 to 1776.0
Generators         33     On-line Capacity      3405.0         -535.0 to 1776.0
Committed Gens     33     Generation (actual)   2901.2              587.4
Loads              17     Load                  2850.0              580.0
  Fixed            17       Fixed               2850.0              580.0
  Dispatchable      0       Dispatchable          -0.0 of -0.0       -0.0
Shunts              1     Shunt (inj)             -0.0             -102.5
Branches           38     Losses (I^2 * Z)        51.25             454.77
Transformers        5     Branch Charging (inj)     -               549.9
Inter-ties         10     Total Inter-tie Flow  1339.8              204.9
Areas               4
```

Figure 7. Power Flow Summary Under Normal Conditions

The total generation capacity is 3405 MW, substantially surpassing the load demand to accommodate system losses, reserve necessities, and dynamic stability. The system losses, totaling 51.25 MW of active power and 454.77 MVAr of reactive power, are within the anticipated parameters for a system of this magnitude.
The surplus generation capacity signifies adequate reserves to provide reliability under normal circumstances or during emergencies.

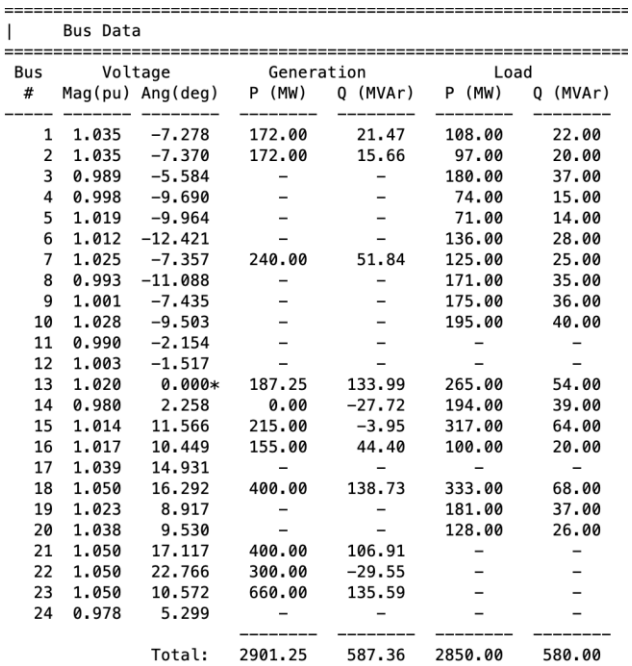

Bus #	Voltage Mag(pu)	Voltage Ang(deg)	Generation P (MW)	Generation Q (MVAr)	Load P (MW)	Load Q (MVAr)
1	1.035	-7.278	172.00	21.47	108.00	22.00
2	1.035	-7.370	172.00	15.66	97.00	20.00
3	0.989	-5.584	-	-	180.00	37.00
4	0.998	-9.690	-	-	74.00	15.00
5	1.019	-9.964	-	-	71.00	14.00
6	1.012	-12.421	-	-	136.00	28.00
7	1.025	-7.357	240.00	51.84	125.00	25.00
8	0.993	-11.088	-	-	171.00	35.00
9	1.001	-7.435	-	-	175.00	36.00
10	1.028	-9.503	-	-	195.00	40.00
11	0.990	-2.154	-	-	-	-
12	1.003	-1.517	-	-	-	-
13	1.020	0.000*	187.25	133.99	265.00	54.00
14	0.980	2.258	0.00	-27.72	194.00	39.00
15	1.014	11.566	215.00	-3.95	317.00	64.00
16	1.017	10.449	155.00	44.40	100.00	20.00
17	1.039	14.931	-	-	-	-
18	1.050	16.292	400.00	138.73	333.00	68.00
19	1.023	8.917	-	-	181.00	37.00
20	1.038	9.530	-	-	128.00	26.00
21	1.050	17.117	400.00	106.91	-	-
22	1.050	22.766	300.00	-29.55	-	-
23	1.050	10.572	660.00	135.59	-	-
24	0.978	5.299	-	-	-	-
		Total:	2901.25	587.36	2850.00	580.00

Figure 8. Bus Data Smulation

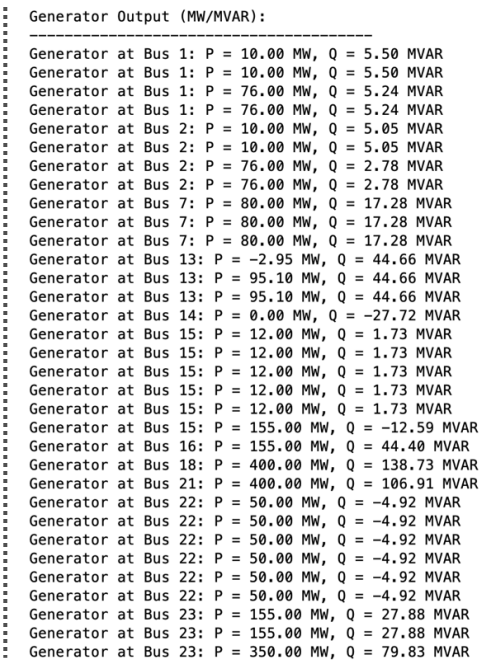

```
Generator Output (MW/MVAR):
---------------------------------------
Generator at Bus 1: P = 10.00 MW, Q = 5.50 MVAR
Generator at Bus 1: P = 10.00 MW, Q = 5.50 MVAR
Generator at Bus 1: P = 76.00 MW, Q = 5.24 MVAR
Generator at Bus 1: P = 76.00 MW, Q = 5.24 MVAR
Generator at Bus 2: P = 10.00 MW, Q = 5.05 MVAR
Generator at Bus 2: P = 10.00 MW, Q = 5.05 MVAR
Generator at Bus 2: P = 76.00 MW, Q = 2.78 MVAR
Generator at Bus 2: P = 76.00 MW, Q = 2.78 MVAR
Generator at Bus 7: P = 80.00 MW, Q = 17.28 MVAR
Generator at Bus 7: P = 80.00 MW, Q = 17.28 MVAR
Generator at Bus 7: P = 80.00 MW, Q = 17.28 MVAR
Generator at Bus 13: P = -2.95 MW, Q = 44.66 MVAR
Generator at Bus 13: P = 95.10 MW, Q = 44.66 MVAR
Generator at Bus 13: P = 95.10 MW, Q = 44.66 MVAR
Generator at Bus 14: P = 0.00 MW, Q = -27.72 MVAR
Generator at Bus 15: P = 12.00 MW, Q = 1.73 MVAR
Generator at Bus 15: P = 12.00 MW, Q = 1.73 MVAR
Generator at Bus 15: P = 12.00 MW, Q = 1.73 MVAR
Generator at Bus 15: P = 12.00 MW, Q = 1.73 MVAR
Generator at Bus 15: P = 12.00 MW, Q = 1.73 MVAR
Generator at Bus 15: P = 155.00 MW, Q = -12.59 MVAR
Generator at Bus 16: P = 155.00 MW, Q = 44.40 MVAR
Generator at Bus 18: P = 400.00 MW, Q = 138.73 MVAR
Generator at Bus 21: P = 400.00 MW, Q = 106.91 MVAR
Generator at Bus 22: P = 50.00 MW, Q = -4.92 MVAR
Generator at Bus 22: P = 50.00 MW, Q = -4.92 MVAR
Generator at Bus 22: P = 50.00 MW, Q = -4.92 MVAR
Generator at Bus 22: P = 50.00 MW, Q = -4.92 MVAR
Generator at Bus 22: P = 50.00 MW, Q = -4.92 MVAR
Generator at Bus 22: P = 50.00 MW, Q = -4.92 MVAR
Generator at Bus 23: P = 155.00 MW, Q = 27.88 MVAR
Generator at Bus 23: P = 155.00 MW, Q = 27.88 MVAR
Generator at Bus 23: P = 350.00 MW, Q = 79.83 MVAR
```

Figure 9. Generator Output Results

The principal findings from the bus data include voltage magnitudes which vary from 0.978 p.u. [bus 24] to 1.050 p.u. [buses: 18,21,22,23]. The majority of buses function within an acceptable range of ±5% from the nominal voltage of 1.0 p.u., hence maintaining stability throughout the network. Another key observation is taken upon voltage angles which exhibit considerable variation, ranging from -12.42° [bus 6] to 22.77° [bus 22]. The negative angles at certain buses signify the direction of power flow towards load centers, whilst positive angles denote power sources or upstream buses. Buses linked to generators, specifically Bus 18 and Bus 23, demonstrate robust voltage support, with values at the maximum threshold of operating norms.

Overall, the voltage magnitudes indicate that the network functions effectively with negligible voltage dips, and the angles correspond with anticipated power flow patterns.

Generator Output:

The system comprises 33 generators allocated among 10 generator buses, yielding a total of 2901.2 MW of active power and 587.4 MVAr of reactive power. The examination of individual generator contributions indicates that bus 1 contains 4 generators with a cumulative output of 172 MW. Route 23 functions as a principal generation hub with three generators delivering 660 MW, rendering it essential for system power stabilization. Both of the buses 18 and 21 deliver 400 MW, offering substantial assistance in fulfilling the system's total load need.

When it comes to reactive power contributions, the most reactive power injection occurs at bus 18 [138.73 MVAr], indicating its significance in sustaining voltage stability for adjacent loads.The generators at Bus 23 collectively provide substantial reactive power, hence maintaining stability in one of the system's most vital areas.

Generators are effectively employed to sustain load equilibrium while addressing reactive power requirements and system losses.
The injections of reactive power significantly enhance voltage stability throughout the network, especially at buses experiencing elevated loads or transmission losses.

Branch Power Flow Analysis

Figure 10 depict branch power flow data. The power traverses the network's 38 transmission lines and transformers, which are essential for comprehending energy distribution. The connection between bus 3 and bus 24 transmits the maximum active power flow of 212.32 MW, underscoring its significance in load distribution. Numerous additional branches demonstrate substantial power transfers, especially those linking high-load buses or principal generation centers. Reactive power flows are significantly elevated on extended transmission lines, with the segment between bus 17 and bus 22 demonstrating a reactive power loss of 26.31 MVAr. The cumulative active power losses throughout the network total 51.25 MW, predominantly attributable to line resistance. The total reactive power losses amount to 454.77 MVAr, predominantly occurring in lines characterized by elevated inductive reactance.

Branch Data								
Brnch #	From Bus	To Bus	From Bus Injection P (MW)	From Bus Injection Q (MVAr)	To Bus Injection P (MW)	To Bus Injection Q (MVAr)	Loss (I^2 * Z) P (MW)	Loss (I^2 * Z) Q (MVAr)
1	1	2	11.94	-26.92	-11.94	-22.45	0.004	0.02
2	1	3	-7.97	21.57	8.31	-26.11	0.342	1.32
3	1	5	60.03	4.83	-59.29	-4.37	0.741	2.87
4	2	4	38.44	19.15	-37.85	-20.43	0.587	2.27
5	2	6	48.50	-1.04	-47.41	-0.19	1.093	4.22
6	3	9	22.90	-17.01	-22.66	14.75	0.240	0.93
7	3	24	-211.21	6.12	212.32	34.48	1.113	40.60
8	4	9	-36.15	5.43	36.52	-6.83	0.364	1.41
9	5	10	-11.71	-9.63	11.76	7.30	0.046	0.18
10	6	10	-88.59	-130.31	89.66	-121.12	1.067	4.64
11	7	8	115.00	26.84	-112.88	-20.35	2.118	8.18
12	8	9	-36.92	3.36	37.53	-5.46	0.604	2.34
13	8	10	-21.19	-18.01	21.50	14.61	0.303	1.17
14	9	11	-105.92	-12.77	106.20	22.87	0.277	10.10
15	9	12	-120.47	-25.69	120.84	39.16	0.369	13.47
16	10	11	-151.18	36.03	151.72	-16.10	0.546	19.93
17	10	12	-166.74	23.18	167.38	0.21	0.641	23.39
18	11	13	-86.15	-54.97	86.76	49.70	0.618	4.82
19	11	14	-171.77	48.19	173.55	-42.96	1.778	13.76
20	12	13	-60.51	-33.30	60.79	25.20	0.271	2.11
21	12	23	-227.70	-6.07	234.10	34.52	6.399	49.85
22	13	23	-225.30	5.10	230.74	17.80	5.438	42.38
23	14	16	-367.55	-23.77	374.60	70.49	7.054	54.88
24	15	16	112.30	-32.60	-112.01	31.13	0.290	2.28
25	15	21	-214.92	-41.97	217.83	53.65	2.913	22.65
26	15	21	-214.92	-41.97	217.83	53.65	2.913	22.65
27	15	24	215.54	48.59	-212.32	-34.48	3.219	24.93
28	16	17	-322.68	-33.86	326.03	54.42	3.353	26.31
29	16	19	115.08	-43.35	-114.65	41.64	0.433	3.33
30	17	18	-186.94	-58.69	187.58	60.49	0.638	5.10
31	17	22	-139.09	4.28	141.54	-9.26	2.454	19.14
32	18	21	-60.29	5.12	60.40	-10.26	0.111	0.87
33	18	21	-60.29	5.12	60.40	-10.26	0.111	0.87
34	19	20	-33.17	-39.32	33.29	31.34	0.113	0.88
35	19	20	-33.17	-39.32	33.29	31.34	0.113	0.88
36	20	23	-97.29	-44.34	97.58	41.63	0.291	2.25
37	20	23	-97.29	-44.34	97.58	41.63	0.291	2.25
38	21	22	-156.46	20.12	158.46	-20.29	1.994	15.54
						Total:	51.246	454.77

Load Flow Analysis Successful

Figure 10. Branch Data Power Flow Simulation

As a result, we can state that the branch power flows validate that the network efficiently transmits power between generation hubs and load centers, with losses maintained within acceptable thresholds.

The system's voltage stability and load balancing capabilities demonstrate a resilient architecture adept at managing operating requirements and minor disruptions. The allocation of reactive power support guarantees that voltage fluctuations are reduced throughout the network.

Figure 11 is a MATLAB visualisation of our IEEE-24 Bus System under normal conditions in the form of the graph. Green nodes indicate generator buses, while blue nodes represent either load or transmission buses. The edges between nodes represent the transmission lines or transformers that interconnect the buses. The layout demonstrates a meshed network where multiple paths exist between different nodes, enhancing system reliability and resilience.The central portion of the network shows higher connectivity, where critical buses play a role in balancing power flow.

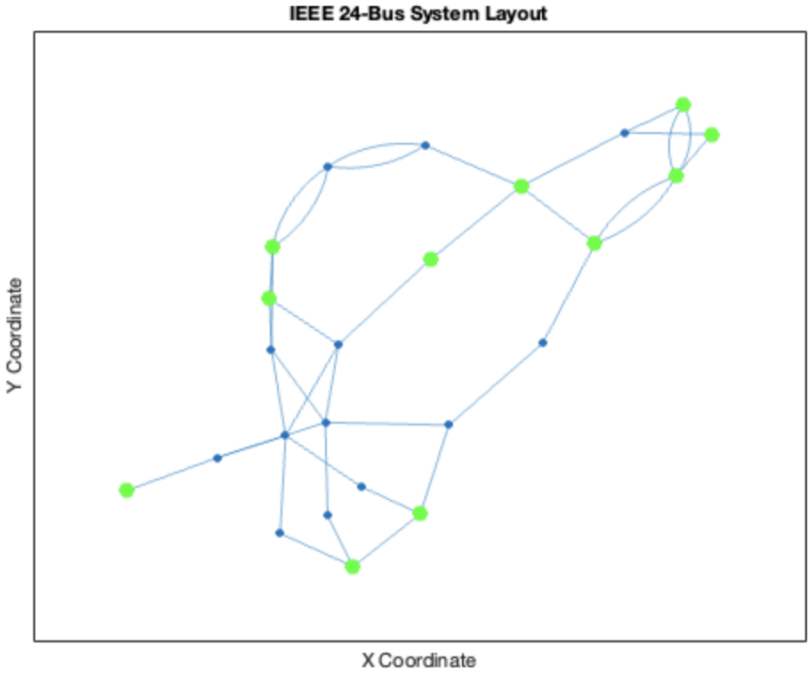

Figure 11. IEEE-24 Bus System Layout

B. Fragility Curves Utilization for IEEE-24 Bus System

Fragility curves for the IEEE 24-Bus System were produced in MATLAB using parameters that were introduced in [3] and can be found in the following table.

Damage State	PGA Median	Standard Deviation
slight	0.4	0.3
moderate	0.6	0.3
extensive	0.8	0.3
complete	1.0	0.3

Table 3. Parameters of Damage States

The values for the median and standard deviation were derived from empirical studies, which indicate that these parameters are commonly used for developing fragility curves in power system analysis. The illustration of the curves is represented in the figure 12.

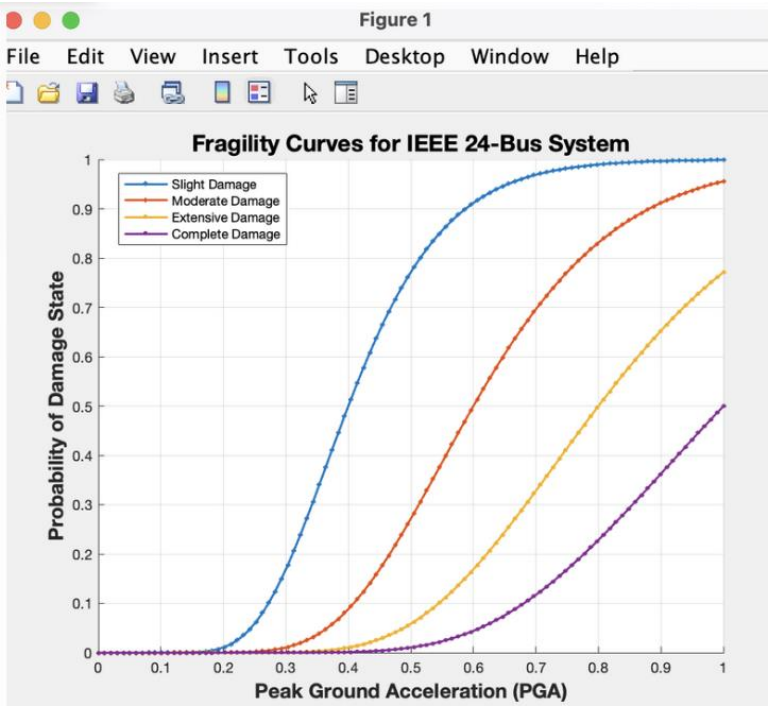

Figure 12. Fragility Curves for IEEE-24 Bus System

Figure 12 provide a clear visualisation signifying the possibility of these damage stages being attained or surpassed as the PGA escalates. For the Slight Damage curve, the probability begins to increase markedly at roughly PGA 0.2 and approaches certainty at around PGA 0.4. This trend suggests that the majority of components within the system are susceptible to minor seismic occurrences, leading to minimal damage. The significant rise in likelihood indicates that this state is the most probable outcome at low earthquake intensity. The Moderate Damage curve commences its rise later, commencing at roughly PGA 0.4 and approaching certainty at PGA 0.6. This incremental rise underscores the system's ability to endure mild seismic forces, with this damage state prevailing only at marginally elevated PGA levels. The Extensive Damage curve becomes significant at PGA values beyond 0.5 and approaches a near-certain likelihood at PGA 0.8. This signifies that significant effects on the system components arise solely during intense earthquake forces. The gradual initial ascent of this curve indicates that the majority of components exhibit resistance to such damage levels at moderate PGA values. The Complete Damage curve begins to rise with PGA levels exceeding 0.7, with probabilities reaching substantial only at PGA 1.0. This graph indicates that catastrophic failures are rare and transpire solely under severe earthquake intensities. The delayed ascent and subdued form of this curve suggest a considerable resilience of the system to complete breakdowns. Notable observations encompass the gradual divergence of the curves, indicating the escalating severity of damage with elevated PGA values. The pronounced inclines of the Slight and Moderate Damage curves indicate a more predictable

occurrence, whilst the gentler inclines of the Extensive and Complete Damage curves signify increased diversity in their manifestation.
For our test system, the fragility curves were incorporated into the modeling framework to detect susceptible buses during seismic events. The likelihood of total damage at a certain PGA was assessed for each bus, and those with a probability beyond a predetermined threshold were identified as vulnerable.

C. PGA & SRI Simulation Results

In the test study, we used 10 earthquake scenarious for simplification and setting examplatory analysis. Figure 13 represents values on how the Peak Ground Acceleration (PGA) impact the System Resilience Index (SRI) across several earthquake scenarios.This investigation illustrates the correlation between seismic intensity and the robustness of the IEEE 24-bus system under defensive islanding settings.

Scenario	PGA	TotalSRI
1	0.66282	80.418
2	0.65265	77.411
3	0.62865	70.412
4	0.74918	106.42
5	0.84116	133.46
6	0.68707	87.662
7	0.86081	138.96
8	0.6571	78.722
9	0.64819	76.099
10	1	173.39

Figure 13. PGA & SRI parameters for each scenario

The investigation reveals PGA values ranging from 0.62865 to 1.0, accompanied by the subsequent major observations. Scenarios 1, 2, 3, 6, 8, and 9 are categorized within the low to moderate range, signifying moderate earthquake intensities. The Total SRI in these scenarios varies from 70.412 to 106.42, indicating moderate resilience with a reduced number of affected components. Scenarios 5, 7, and 10 denote high-intensity seismic events.The Total SRI in these scenarios surpasses 130, with Scenario 10 attaining the peak SRI of 173.39, indicating significant network disruption and heightened isolation needs. The data indicates a robust positive association between PGA and SRI. As PGA escalates, the Total SRI correspondingly increases, indicating the heightened influence of seismic activity on the network.This trend underscores the necessity of integrating adaptive islanding solutions for high-PGA scenarios to preserve stability and operational efficiency.

D. Pre-Isolation Network Visualisation

In each case, the preliminary network configuration was examined to identify susceptible busses. The busses deemed susceptible were marked in red in case of exceeding rate of complete damage,

indicating crucial nodes at risk of failure. This phase is essential for identifying the nodes that necessitate isolation to maintain system stability. Figure 14 shows the most critical scenario with almost all the nodes highlighted in red colour.

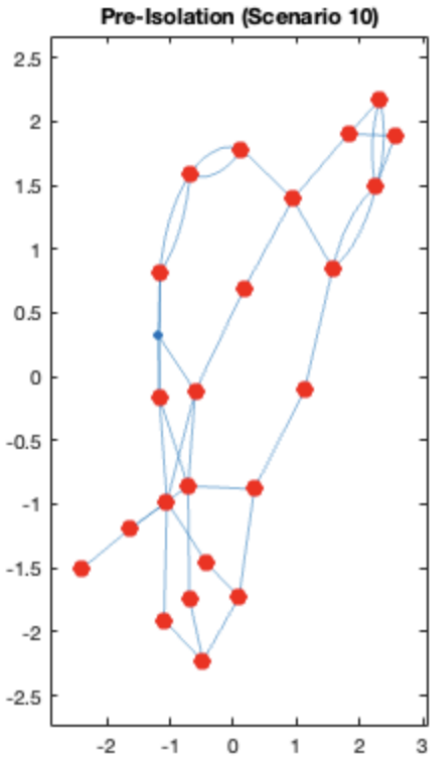

Figure 14. Pre-Isolation Network for Scenario 10

E. Defensive Islanding Using Spectral Clustering

The implementation of spectral clustering for defensive islanding in the IEEE 24-bus system involves following steps:

1. Identifying At-Risk Buses: Fragility curves are used to figure out which buses are vulnerable based on how likely they are to suffer complete damage. A certain percentage of the time, like 40%, is used to decide if a bus is exposed.

2. Island Formation: Spectral clustering divides the power grid into separate islands. The goal is to isolate buses that are at risk while maintaining operational stability in the unaffected parts of the network.

3. Network Adaptation: Transmission lines connected to the vulnerable buses are pointedly removed. This ensures that the isolated islands are self-sufficient, with enough generation to meet local demand.

4. Post-Isolation Load Flow Examination: After the islanding process, the system's performance is re-evaluated using power flow analysis. This ensures that the resultant network structure is stable and viable.

Figure 15 clearly depicts successful implementation of spectral clustering. The power grid is represented as a weighted graph where buses correspond to nodes, and transmission lines are edges. Vulnerable buses are identified based on their probability of damage, derived from fragility curves. The Laplacian matrix is constructed from the graph's adjacency matrix. It captures the connectivity between nodes and reflects the structural dependencies in the network.Eigenvectors of the Laplacian matrix are computed, providing insights into the natural divisions of the graph. The smallest eigenvalues and their corresponding eigenvectors are particularly critical for partitioning. Clusters (or islands) are identified using a k-means clustering algorithm applied to the eigenvectors. Each cluster is designed to maintain internal connectivity while minimizing inter-cluster dependencies.

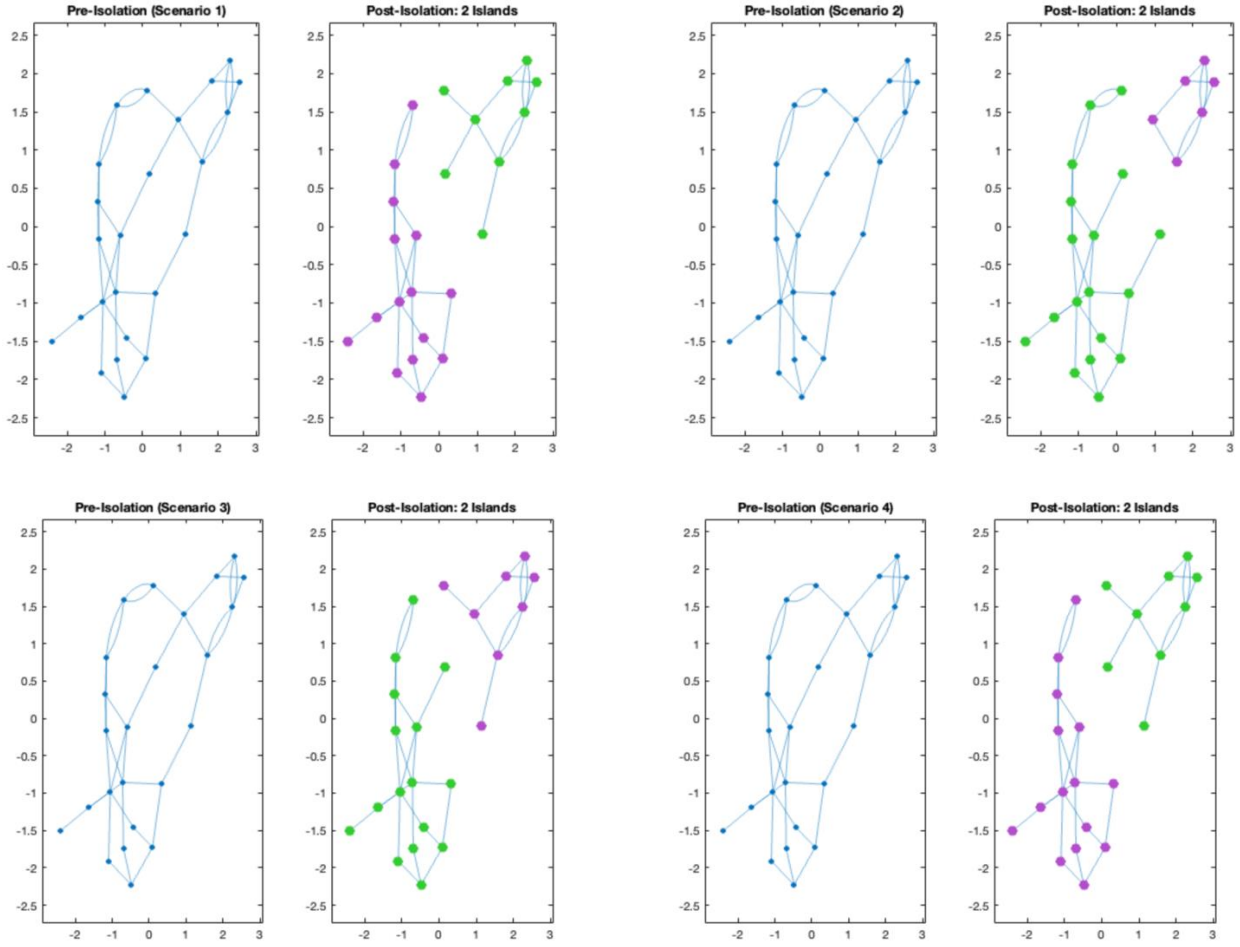

Figure 15.1 Scenarios 1 - 4 for Pre and Post Isolation of Power Grid

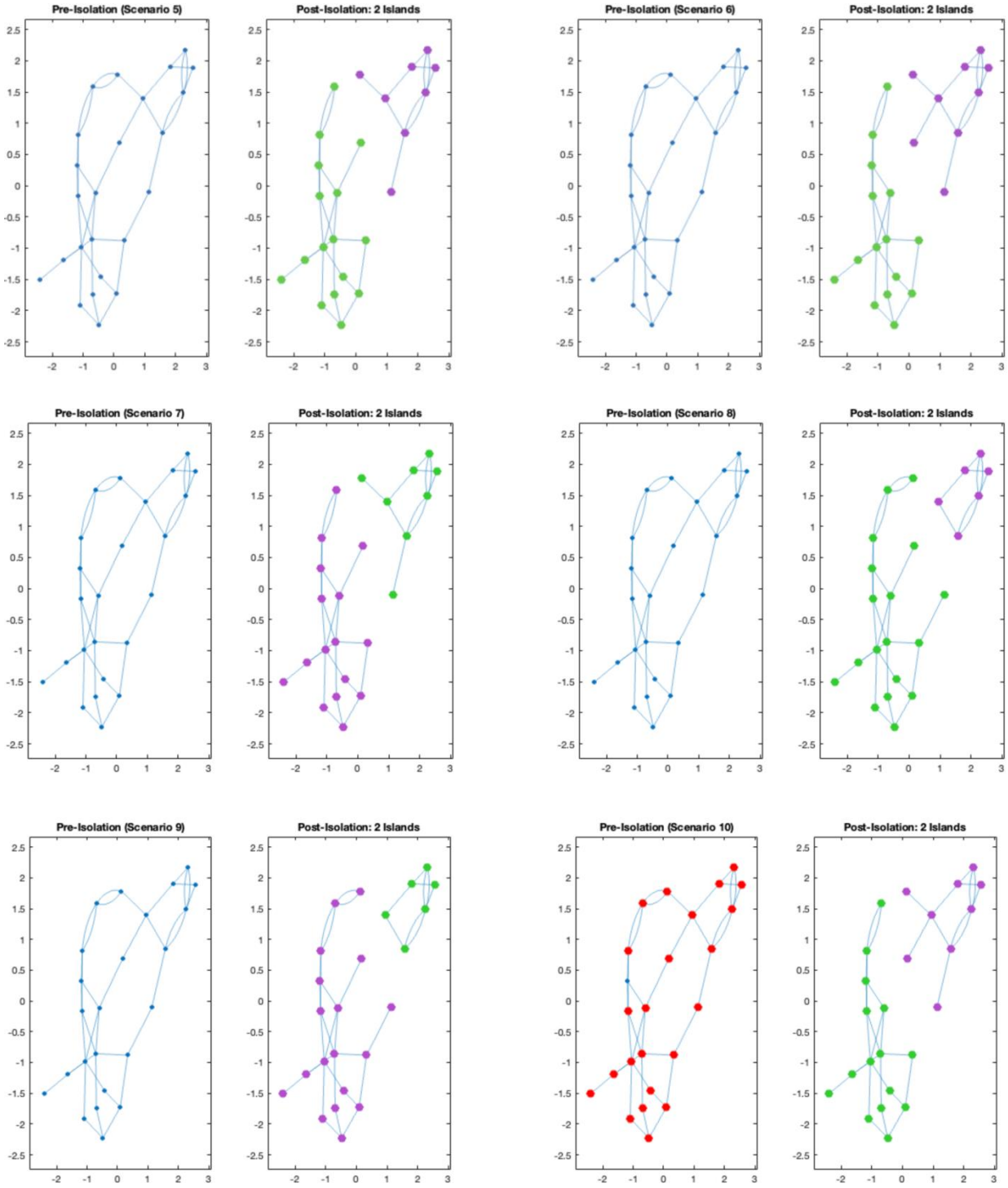

Figure 15.2 Scenarios 5 - 10 Pre and Post Isolation of Networks Using Spectral Clustering

F. Post-Isolation Lad Flow Analysis

The post-isolation load flow analysis examined the effects of defensive islanding on system performance, including changes in branch flows, generator outputs, and system losses. In this section, we include scenario 10 post-isolation analysis as demonstrating changes in load flow for each scenario would be impractical due to the extensive data involved in whole research. The following are the principal observations and behaviors discovered from the analysis.

1. Power Flow Summary

Figure 16 & 17 depict the system summary post-isolation for Scenario 10 for both islands respectevely. Island 1 demonstrates diminished overall generating capacity relative to the pre-isolation network, with active power generation calibrated to satisfy the load and ensure stability. Losses in both active and reactive power remain within permissible limits, demonstrating the effectiveness of the islanding method. Island 2 has a greater reliance on local generation to equilibrate the isolated loads. Active power losses are somewhat increased because to the reduced size and limited interconnections inside the island. Voltage and frequency stability restrictions are well upheld, guaranteeing operational continuity.

```
================================================================================
|     System Summary                                                          |
================================================================================

How many?                How much?              P (MW)            Q (MVAr)
---------------------    --------------------  -------------  -----------------
Buses              15    Total Gen Capacity    1935.0         -225.0 to 890.0
Generators         17    On-line Capacity      1935.0         -225.0 to 890.0
Committed Gens     17    Generation (actual)   1768.5              433.7
Loads              12    Load                  1725.0              352.0
  Fixed            12      Fixed               1725.0              352.0
  Dispatchable      0      Dispatchable          -0.0 of -0.0        -0.0
Shunts              1    Shunt (inj)             -0.0             -100.9
Branches           22    Losses (I^2 * Z)        43.47             387.55
Transformers        4    Branch Charging (inj)     -               406.7
Inter-ties          7    Total Inter-tie Flow    865.4             139.0
Areas               3
```

Figure 16. Post-Isolation Power Flow Summary for Scenario 10 [Island 1]

```
================================================================================
|     System Summary                                                           |
================================================================================

How many?                How much?              P (MW)            Q (MVAr)
---------------------    -------------------  -------------  -----------------
Buses                9     Total Gen Capacity    1470.0         -310.0 to 886.0
Generators          16     On-line Capacity      1470.0         -310.0 to 886.0
Committed Gens      16     Generation (actual)   1156.1              359.8
Loads                5     Load                  1125.0              228.0
  Fixed              5       Fixed               1125.0              228.0
  Dispatchable       0       Dispatchable          -0.0 of -0.0       -0.0
Shunts               0     Shunt (inj)             -0.0                0.0
Branches            12     Losses (I^2 * Z)        31.11             242.69
Transformers         0     Branch Charging (inj)     -               110.9
Inter-ties           2     Total Inter-tie Flow    696.1              67.1
Areas                2
```

Figure 17. Post-Isolation Power Flow Summary for Scenario 10 [Island 2]

2. Bus Voltages

The post-isolation bus voltage magnitudes in both islands demonstrate stable operation, with the majority of buses sustaining values within ±5% of the nominal voltage. Island 1 displays minor discrepancies at essential buses, like Bus 18 and Bus 23, which accommodate substantial generation. These buses are essential for providing voltage support to the rest of the network. In Island 2, the voltage profile is more consistent but exhibits slight declines at buses situated distant from generation centers. The angular differences between the bars indicate a clearly directed power flow to the high load centers, demonstrating load redistribution after isolation.

```
================================================================================
|     Bus Data                                                                 |
================================================================================
 Bus      Voltage          Generation             Load
  #   Mag(pu) Ang(deg)   P (MW)   Q (MVAr)   P (MW)   Q (MVAr)
----- ------- --------  --------  --------  --------  --------
    1  1.035  -18.003    172.00     59.48    108.00     22.00
    2  1.035  -17.828    172.00     30.63     97.00     20.00
    3  0.923  -24.927       -         -      180.00     37.00
    4  0.985  -19.231       -         -       74.00     15.00
    5  1.013  -18.745       -         -       71.00     14.00
    6  1.004  -20.067       -         -      136.00     28.00
    7  1.025  -15.299    240.00     63.57    125.00     25.00
    8  0.986  -18.951       -         -      171.00     35.00
    9  0.979  -16.077       -         -      175.00     36.00
   10  1.018  -16.198       -         -      195.00     40.00
   11  0.980   -8.371       -         -         -         -
   12  0.983   -4.589       -         -         -         -
   13  1.020    0.000*   524.47    181.80    265.00     54.00
   20  1.046   10.174       -         -      128.00     26.00
   23  1.050   10.880    660.00     98.22       -         -
                        --------  --------  --------  --------
              Total:    1768.47    433.71   1725.00    352.00
```

Figure 18. Post-Isolation Bus Data for Scenario 10 [Island 1]

Bus Data						
Bus #	Voltage Mag(pu)	Voltage Ang(deg)	Generation P (MW)	Generation Q (MVAr)	Load P (MW)	Load Q (MVAr)
14	0.980	0.000*	-313.89	58.60	194.00	39.00
15	1.014	14.314	215.00	-89.13	317.00	64.00
16	1.017	11.503	155.00	172.54	100.00	20.00
17	1.038	16.585	-	-	-	-
18	1.050	18.224	400.00	143.54	333.00	68.00
19	1.003	9.211	-	-	181.00	37.00
21	1.050	19.301	400.00	103.07	-	-
22	1.050	24.744	300.00	-28.87	-	-
24	1.017	14.293	-	-	-	-
		Total:	1156.11	359.75	1125.00	228.00

Figure 19. Post-Isolation Bus Data for Scenario 10 [Island 2]

3. Branch Changes

The branch data for scenario 10 show significant changes in the power flow dynamics after the protective islanding, providing important new perspectives on system performance and operational issues on both islands. On island 1, the power redistribution stresses the highly loaded buses, especially the connection between buses 3 and 24, which significantly increases the power transmission on these vital lines. This model shows how well island 1, which generates sources and accommodates most of the high-priority loads, can adapt to maintain service continuity. In particular, on the lines experiencing significantly increased loads, the concentration of power on certain lines raises questions about possible thermal limits and stability margins. This shows that even if island 1 offers the necessary load service, its operational reliability is highly dependent on the capacity of these important branches. In addition, island 1 has higher reactive power flows, especially in the long transmission lines connecting remote buses to central generation plants. Improved reactive power compensation is necessary to control voltage levels and maintain power quality, as increased reactive power flows can cause high voltage sags across the network. The variations in branch flows on Island 1 highlight the need for real-time monitoring and control systems to stop cascading failures when the line is overloaded or voltage is unstable. Island 2, on the other hand, has reduced overall branch flows, reflecting its lower load demand and limited generating capacity. By reducing losses relative to Island 1, power flows are fairly constant over shorter transmission distances. The underutilized branch capacity resulting from the absence of high-demand nodes suggests that the island is not operating at its best. This reduces the likelihood of line overload; however, it results in Island 2 lacking redundancy and flexibility, increasing its vulnerability to further failures. Although less noticeable than on Island 1, the reactive power losses on Island 2 are nonetheless significant given the limited transmission connections connecting its generation and load centres. These losses can impact voltage stability, especially when the island operates for long periods without external support. The limited ability of Island 2

to cope with a large number of faults highlights the need for careful load balancing and effective reactive power management. Analysis of branch data points to a double challenge: while Island 2 is dealing with underutilized capacity and insufficient redundancy, Island 1 suffers from operational stress due to increased branch flows and reactive power losses. These results highlight the need to incorporate advanced optimization techniques—including real-time branch flow changes, load prioritization algorithms, and improved reactive power support—into the protective islanding strategy to ensure stability, efficiency, and reliability of both islands during isolated operations.

Branch Data

Brnch #	From Bus	To Bus	From Bus Injection P (MW)	From Bus Injection Q (MVAr)	To Bus Injection P (MW)	To Bus Injection Q (MVAr)	Loss (I^2 * Z) P (MW)	Loss (I^2 * Z) Q (MVAr)
1	1	2	-22.69	-20.42	22.71	-28.91	0.013	0.07
2	1	3	65.19	38.11	-62.16	-31.89	3.030	11.72
3	1	5	21.51	19.79	-21.32	-21.48	0.184	0.71
4	2	4	28.37	31.65	-27.78	-32.87	0.590	2.28
5	2	6	23.92	7.89	-23.60	-12.07	0.318	1.23
6	3	9	-117.84	-5.11	122.86	21.60	5.022	19.40
7	4	9	-46.22	17.87	46.91	-17.91	0.692	2.68
8	5	10	-49.68	7.48	50.24	-7.76	0.565	2.19
9	6	10	-112.40	-116.82	114.15	-127.04	1.748	7.61
10	7	8	115.00	38.57	-112.76	-31.61	2.237	8.64
11	8	9	-26.36	9.21	26.72	-12.12	0.362	1.40
12	8	10	-31.88	-12.60	32.37	10.02	0.495	1.91
13	9	11	-149.40	-19.07	149.98	40.13	0.577	21.06
14	9	12	-222.09	-8.50	223.34	54.36	1.257	45.86
15	10	11	-157.74	36.76	158.34	-14.66	0.606	22.10
16	10	12	-234.03	48.01	235.34	0.06	1.318	48.07
17	11	13	-308.33	-25.47	314.39	62.82	6.066	47.34
18	12	13	-174.58	-51.77	176.64	57.84	2.062	16.09
19	12	23	-284.11	-2.65	294.47	62.36	10.361	80.72
20	13	23	-231.57	7.14	237.32	18.20	5.750	44.81
21	20	23	-64.00	-13.00	64.11	8.83	0.108	0.83
22	20	23	-64.00	-13.00	64.11	8.83	0.108	0.83
						Total:	43.469	387.55

Figure 20. Post-Isolation Branch Data for Scenario 10 [Island 1]

Branch Data								
Brnch #	From Bus	To Bus	From Bus Injection P (MW)	From Bus Injection Q (MVAr)	To Bus Injection P (MW)	To Bus Injection Q (MVAr)	Loss (I^2 * Z) P (MW)	Loss (I^2 * Z) Q (MVAr)
1	14	16	-507.89	19.60	521.35	76.95	13.458	104.70
2	15	16	286.40	-48.70	-284.59	59.12	1.802	14.17
3	15	21	-194.20	-46.60	196.61	54.41	2.415	18.79
4	15	21	-194.20	-46.60	196.61	54.41	2.415	18.79
5	15	24	0.00	-11.23	0.00	0.00	0.002	0.02
6	16	17	-363.76	-23.38	368.00	50.86	4.235	33.24
7	16	19	182.01	39.85	-181.00	-37.00	1.013	7.80
8	17	18	-223.32	-56.26	224.21	60.02	0.883	7.06
9	17	22	-144.68	5.39	147.34	-8.76	2.660	20.74
10	18	21	-78.60	7.76	78.79	-12.29	0.188	1.48
11	18	21	-78.60	7.76	78.79	-12.29	0.188	1.48
12	21	22	-150.81	18.83	152.66	-20.11	1.851	14.42
							---	---
						Total:	31.111	242.69

Figure 21. Post-Isolation Branch Data for Scenario 10 [Island 2]

4. Performance Assessment

Table 4 highlights the performance assessment for Scenario 10 after whole analysis on pre-isolated and post-isolated networks has been implemented.

Metric	Pre-Isolation	Post-Isolation	Performance Indicator
Total Generation Capacity (MW)	2901,25	1768,47	-39,05%
Total Load (MW)	2850	1725	-39,47%
Branches Removed	-	16	16 branches removed
Voltage Stability	Stable	Reduced Stability	Decreased
Power Losses Reduction	-	43,47W	-43.47 MW

Table 4. Performance Assessment

Following isolation, the general generating capacity and load were much reduced, suggesting the disconnection of sensitive buses and associated components. The capacity lowering assured that the surviving network could operate safely free from seismic risk. When the system was isolated, the number of branches dropped since links to the dead buses were removed to maintain the general network integrity. The change in network architecture influenced the distribution of electricity, therefore reducing the access to power sources in some areas. Although maintained before to isolation, voltage stability suffered post-isolation settings because of changed power flow

pathways and reduced generating capacity. This emphasizes a major trade-off in defensive islanding: whereas the network develops resilience against cascading failures, maintaining ideal voltage levels presents operational challenges. The table also shows the effectiveness of the post-isolation network since power losses limited to a smaller grid. This suggests that the operational grid may distribute electricity more effectively even in areas that are separated even. While pointing areas for possible improvement in post-isolation performance, such voltage stability maintenance and capacity reduction minimizing, the chart also shows the effectiveness of defensive islanding in safeguarding the network.

CHAPTER FIVE

DISCUSSION AND CONCLUSIONS

In this research, we demonstrated the implementation and effectiveness of islanding measures to improve power system resilience during seismic events. The study of the IEEE 24-bus system in several scenarios, especially scenario 10, provided significant insights into the system behavior during and after isolation. The thorough analysis revealed several important points spanning hazard characterization and seismic modeling to islanding performance. The islanding approach effectively detected and isolated vulnerable components, resulting in a network restructuring that maintained operational stability.Fragility curves generated for this study using empirical seismic vulnerability criteria provided a solid basis for assessing the likelihood of damage states in different PGAs. Deterministic earthquake modeling highlighted key thresholds at which buses and branches became vulnerable. For instance, Scenario 10 showed how defensive islanding can help keep service going in parts of the network that aren't being affected as much.
The study has effectively illustrated the implementation of defensive islanding as a method for augmenting the resilience of power networks during seismic occurrences. The constructed fragility curves accurately represented the seismic susceptibility of the IEEE 24-bus system. The defensive islanding method maintained operational stability and reduced cascade failures in post-isolation situations. Post-isolation studies indicated substantial decreases in system inefficiencies (e.g., losses) while preserving acceptable voltage stability levels.
Practical Considerations are as followed:

- Resilience Enhancement: The methodology outlined in this thesis provides a practical foundation for the implementation of defensive islanding in actual power systems, especially in areas susceptible to seismic events.
- System Efficiency: The noted decrease in system losses following isolation highlights the capacity of defensive islanding to enhance overall network efficiency, even under standard operational conditions.
- Future Scalability: Although this study concentrated on the IEEE 24-bus system, the concept is applicable to larger systems with more intricate configurations. Also, the number of scenarios can be escalated per needed parameters.

The integration of defensive islanding methods with real-time seismic monitoring systems should be the main focus of further studies and useful applications. This integration would help dynamic and automatic reaction systems to enable the power system to react fast to seismic shocks. By use of real-time data comprising ground motion intensity and frequency, the system may generate

adaptive judgments to isolate sensitive components and prevent cascading failures. By increasing situational awareness for operators, this link helps them to better monitor and run the post-isolation network. Additionally using cloud-based platforms and Internet of Things (IoT) technologies could improve data collecting, processing speed, and general system responsiveness. Althought this paper stresses the technical aspects of defensive islanding and post-isolation performance, it is vital and equailly important to aress the need of evaluating the financial consequences of the recommended approach. Additional studies could help to assess the cost-benefit trade-offs connected to reduced power losses, improved system dependability, and minimized damages. Studies should especially focus on estimating prospective operating cost reductions, lowering service interruptions, and lowering long-term maintenance costs resulting from better resilience. Establishing a comprehensive economic framework will help utilities and stakeholders to have necessary measurements to support the investment in defensive islanding technology and its application with present systems.

The current model mostly relies on generalized fragility curves using median and standard deviation values for damage state projections. Other fragility factors should be included into future research to improve the accuracy of these projections. Factors could include design criteria, equipment age, past performance, environmental influences including soil conditions and weathering effects. Incorporating mentioned properties into fragility analysis will help to evaluate the system's vulnerability with more accuracy. For example, outdated tools or components built under outmoded design criteria could show different damage thresholds than newer, more robust installations. This thorough modeling helps to improve forecast accuracy and enable tailoring of mitigating strategies for specific system setups.

These suggestions assure their conformance with operational criteria and growing concerns in power system management, so improving the actual execution and robustness of defensive islanding approaches.

Finally, defensive islanding is a practical and effective way to minimize the consequences of seismic events on power systems. Guaranteeing operational stability and efficiency helps to support the main goal of building strong infrastructure against natural disasters.

CHAPTER SIX

REFERENCES

[1] S. Liasi, N. S. Ghiasi and R. Hadidi, "An Evaluative Framework for Regional Vulnerability and Power System Resilience Against Earthquakes: A Case Study of Charleston County, South Carolina," *2023 IEEE 3rd International Conference on Digital Twins and Parallel Intelligence (DTPI)*, Orlando, FL, USA, 2023, pp. 1-6.

[2] E. Sahnur Nasution, S. Syahrial, I. Devi Sara and Y. Away, "State of The Art: Fragility Function of Electrical Power System," 2023 6th International Seminar on Research of Information Technology and Intelligent Systems (ISRITI), Batam, Indonesia, 2023, pp.260-265

[3] M. Nazemi and P. Dehghanian, "Seismic-Resilient Bulk Power Grids: Hazard Characterization, Modeling, and Mitigation," in IEEE Transactions on Engineering Management, vol. 67, no. 3, pp. 614-630, Aug. 2020

[4] Lifshitz Sherzer, G.; Urlainis, A.; Moyal, S.; Shohet, I.M. "Seismic Resilience in Critical Infrastructures: A Power Station Preparedness Case Study". *Appl. Sci.* 2024, *14*, 3835.

[5] National Public Radio (NPR). (2023, February 9). "The deadliest earthquakes in history". Retrieved December 23, 2024, from [https://www.npr.org/2023/02/09/1155836898/deadliest-earthquakes list]

[6] M. H. Oboudi, M. Mohammadi, D. N. Trakas and N. D. Hatziargyriou, "A Systematic Method for Power System Hardening to Increase Resilience Against Earthquakes," in IEEE Systems Journal, vol. 15, no. 4, pp. 4970-4979, Dec. 2021.18

[7] M. Ahmadi, M. Bahrami, M. Vakilian and M. Lehtonen, "Application of Hardening Strategies and DG Placement to Improve Distribution Network Resilience against Earthquakes," 2020 IEEE PES Transmission & Distribution Conference and Exhibition - Latin America (T&D LA), Montevideo, Uruguay, 2020, pp. 1-6.

[8] ST-Risk. (n.d.). Fragility curve development with HAZUS. Retrieved December 23, 2024, from [http://www.st-risk.com/tech_HAZUS.html]

[9] H. Liang and Q. Xie, "System Vulnerability Analysis Simulation Model for Substation Subjected to Earthquakes," in IEEE Transactions on Power Delivery, vol. 37, no. 4, pp. 2684-2692, Aug. 2022.

[10] Y. Zheng et al., "The Resilience Assessment Method of Electric-gas System under Earthquake Disaster," 2020 IEEE 3rd Student Conference on Electrical Machines and Systems (SCEMS), Jinan, China, 2020, pp. 591-595.

[11] Y. Jin, M. Xia, Q. Chen and Y. Xian, "Research on Emergency Assessment and Recovery Strategy of Highway Energy System Based on Earthquake Disaster Scenario," 2023 IEEE/IAS Industrial and Commercial Power System Asia (I&CPS Asia), Chongqing, China, 2023, pp. 1654-1659.
[12] A. Pan, Y. Zhang, Y. Sun, L. Zhang, J. Wu and X. Yang, "Scenario construction and vulnerability mitigation of natural hazards-triggered power grid incidents," 2024 9th Asia Conference on Power and Electrical Engineering (ACPEE), Shanghai, China, 2024, pp. 1768-1773.

[13] Li, X.; Xie, Q.; Wen, J. "Seismic Performance Evaluation and Retrofit Strategy of Overhead Gas-Insulated Transmission Lines." *Buildings* 2023, *13*, 2968.19

[14] Y. Shen, C. Gu, X. Yang and P. Zhao, "Impact Analysis of Seismic Events on Integrated Electricity and Natural Gas Systems," in IEEE Transactions on Power Delivery, vol. 36, no. 4, pp. 1923-1931, Aug. 2021.

[15] M. Carratù, V. Gallo, V. Paciello and A. Pietrosanto, "A deep learning approach for the development of an Early Earthquake Warning system," 2022 IEEE International Instrumentation and Measurement Technology Conference (I2MTC), Ottawa, ON, Canada, 2022, pp. 1-6.

[16] S. Yujun, P. Chunmei and L. Yue, "Construction of Disaster Prevention and Reduction Safety Barrier of Power Grid Based on Power Internet of Things Technology," 2023 Panda Forum on Power and Energy (PandaFPE), Chengdu, China, 2023, pp. 1344-1349.

[17] Y. Sherki, N. Gaikwad, J. Chandle and A. Kulkarni, "Design of real time sensor system for detection and processing of seismic waves for earthquake early warning system," 2015 International Conference on Power and Advanced Control Engineering (ICPACE), Bengaluru, India, 2015, pp. 285-289.

[18] R. M. Labanan, B. S. Fabito and R. C. Raga, "Development of an on-Site Earthquake Early Warning System for one Private Higher Educational Institution (HEI) and Its Nearby Community in Manila, Philippines," 2022 International Conference on Computer Applications Technology (CCAT), Guangzhou, China, 2022, pp. 34-39.

[19] P. Pierleoni, A. Belli, M. Esposito, R. Concetti and L. Palma, "Earthquake Early Warning Services Based on Very Low-Cost Internet of Things Devices," 2022 61st FITCE International Congress Future Telecommunications: Infrastructure and Sustainability (FITCE), Rome, Italy, 2022, pp. 1-5.20

[20] J. J. McGuire, D. E. Smith, A. D. Frankel, E. A. Wirth, S. K. McBride, and R. M. de Groot, "Expected warning times from the ShakeAlert earthquake early warning system for earthquakes in the pacific northwest," 2021.

[21] R. Weinmann, T. K. A. Brekken and E. Cotilla-Sanchez, "Impacts of Remedial Action Schemes on Power System Resilience After Large-Scale Earthquakes," 2023 International Conference on Smart Energy Systems and Technologies (SEST), Mugla, Turkiye, 2023, pp. 1-6.

[22] A. Privadi, D. R. Damara, P. L. Widati and F. R. Triputra, "Indonesia's Cable Based Tsunameter (CBT) System as an Earthquake Disaster Mitigation System in East Nusa Tenggara," 2021 IEEE Ocean Engineering Technology and Innovation Conference: Ocean Observation, Technology and Innovation in Support of Ocean Decade of Science (OETIC), Jakarta, Indonesia, 2021, pp. 63-67.

[23] N. Germenis, P. Fountas and C. Koulamas, "Low Latency and Low Cost Smart Embedded Seismograph for Early Warning IoT Applications," 2020 9th Mediterranean Conference on Embedded Computing (MECO), Budva, Montenegro, 2020, pp. 1-4.

[24] P. Pierleoni et al., "Performance Evaluation of a Low-Cost Sensing Unit for Seismic Applications: Field Testing During Seismic Events of 2016-2017 in Central Italy," in IEEE Sensors Journal, vol. 18, no. 16, pp. 6644-6659, Aug.15, 2018,

[25] S. S. Kiran, N. Vagdevi, M. V. Devarao, M. K. Babu and K. S. V. L. N. Swamy, "Predicting Earthquake by using GPS Seismology and GNSS Based System," 2022 International Conference on Computing, Communication and Power Technology (IC3P), Visakhapatnam, India, 2022, pp. 199-203.21

[26] K. Su and S. Jin, "Real-Time Seismic Waveforms Estimation of the 2019 MW = 6.4 and Mw = 7.1 California Earthquakes With High-Rate Multi-GNSS Observations," in IEEE Access, vol. 8, pp. 85411-85420, 2020.

[27] M. R. Kibria Badhon, A. Ranjan Barai and F. Zhora, "Remote Real Time Monitoring and Safety System for Earthquake and Fire Detection Based on Internet of Things," 2019 3rd International Conference on Electrical, Computer & Telecommunication Engineering (ICECTE), Rajshahi, Bangladesh, 2019, pp. 41-44.

[28] Y. Wu et al., "A Rapid Recovery Strategy for Post-Earthquake Power Grids with the Auxiliary Support of V2G," 2022 IEEE/IAS Industrial and Commercial Power System Asia (I&CPS Asia), Shanghai, China, 2022, pp. 1680-1685.

[29] C. Deng, Z. Xue, K. Wang, Q. Zhang and C. Zou, "A Resilience-Based Post-Earthquake Restoration Method for Multi-State Power Distribution Networks," 2023 Panda Forum on Power and Energy (PandaFPE), Chengdu, China, 2023, pp. 2221-2225.

[30] M. Panteli, D. N. Trakas, P. Mancarella and N. D. Hatziargyriou, "Boosting the Power Grid Resilience to Extreme Weather Events Using Defensive Islanding," in IEEE Transactions on Smart Grid, vol. 7, no. 6, pp. 2913-2922, Nov. 2016.

[31] S. Qazi and W. Young, "Disaster relief management and resilience using photovoltaic energy," 2014 International Conference on Collaboration Technologies and Systems (CTS), Minneapolis, MN, USA, 2014, pp. 628-632.

[32] W. Zhu, M. Wu, Q. Xie and Y. Chen, "Post-Earthquake Rapid Assessment Method for Electrical Function of Equipment in Substations," in IEEE Transactions on Power Delivery, vol. 38, no. 5, pp. 3312-3321, Oct. 2023.22

[33] M. Saltos-Rodríguez, A. Velásquez-Lozano, D. Ortiz-Villalba, G. Llumigusín-Cachipuz and J. Yánez-Chancusig, "Power Distribution System Outage Management by Natural Disasters with Optimizing of Resource and Restoration," 2022 IEEE Sixth Ecuador Technical Chapters Meeting (ETCM), Quito, Ecuador, 2022, pp. 1-6.

[34] Y. Xu, S. Tang, Y. Zhang, H. Han, P. Zhang and C. Sui, "Research on the method of emergency strategy generation for city power grid system destruction," 2022 IEEE 2nd International Conference on Data Science and Computer Application (ICDSCA), Dalian, China, 2022, pp. 172-175.

[35] N. R. Romero, L. K. Nozick, I. D. Dobson, N. Xu and D. A. Jones, "Transmission and Generation Expansion to Mitigate Seismic Risk," in IEEE Transactions on Power Systems, vol. 28, no. 4, pp. 3692-3701, Nov. 2013.

[36] Y. Qiu, Q. Li, J. Yu, D. Wang and S. Zhang, "Probability Based Vulnerability Analysis of UHVDC Supported Filter Circuit Under Earthquakes," 2023 IEEE 7th Conference on Energy Internet and Energy System Integration (EI2), Hangzhou, China, 2023, pp. 5335-5340.

[37] H. Li, J. Peng, Z. Xv, J. Feng and H. Liang, "Seismic Vulnerability Analysis of High Voltage Power Transformer," 2021 Power System and Green Energy Conference (PSGEC), Shanghai, China, 2021, pp. 593-598.

[38] Z. Yang, P. Dehghanian and M. Nazemi, "Seismic-Resilient Electric Power Distribution Systems: Harnessing the Mobility of Power Sources," in IEEE Transactions on Industry Applications, vol. 56, no. 3, pp. 2304-2313, May-June 202023

[39] Urlainis, A.; Shohet, I.M. “A Comprehensive Approach to Earthquake-Resilient Infrastructure: Integrating Maintenance with Seismic Fragility Curves.” *Buildings* 2023,*13*,2265.

[40] A. Serrano-Fontova et al., "A Comprehensive Review and Comparison of the Fragility Curves Used for Resilience Assessments in Power Systems," in IEEE Access, vol. 11, pp. 108050-108067, 2023.

[41] M. Panteli and P. Mancarella, "Operational resilience assessment of power systems under extreme weather and loading conditions," 2015 IEEE Power & Energy Society General Meeting, Denver, CO, USA, 2015, pp. 1-5.

[42] J. Guenaou, P. Henneaux and D. S. Kirschen, "Impact of distributed energy resources on power system resilience against earthquakes," 2022 IEEE PES Innovative Smart Grid Technologies Conference Europe (ISGT-Europe), Novi Sad, Serbia, 2022, pp. 1-5.

[43] A. Mate, T. Hagan, E. Cotilla-Sanchez, T. K. A. Brekken and A. Von Jouanne, "Impacts of Earthquakes on Electrical Grid Resilience," 2021 IEEE/IAS 57th Industrial and Commercial Power Systems Technical Conference (I&CPS), Las Vegas, NV, USA, 2021, pp. 1-5. [44] S. Mohagheghi and P. Javanbakht, "Power Grid and Natural Disasters: A Framework for Vulnerability Assessment," 2015 Seventh Annual IEEE Green Technologies Conference, New Orleans, LA, USA, 2015, pp. 199-205.

[45] M. A. Mohamed, T. Chen, W. Su and T. Jin, "Proactive Resilience of Power Systems Against Natural Disasters: A Literature Review," in IEEE Access, vol. 7, pp. 163778-163795, 2019.24

[46] M. S. Miah, R. Shah, N. Amjady, T. Surinkaew and S. Islam, "Resiliency Assessment and Enhancement of Renewable Dominated Edge of Grid Under High-Impact Low-Probability Events—A Review," in IEEE Transactions on Industry Applications.

[47] C. Ozen and K. Kaya, "Earthquake Effects on Electricity Network: A Case Study in Turkish Grid," 2023 5th Global Power, Energy and Communication Conference (GPECOM), Nevsehir, Turkiye, 2023, pp. 333-338.

[48] H. Liang and Q. Xie, "Resilience-Based Sequential Recovery Planning for Substations Subjected to Earthquakes," in IEEE Transactions on Power Delivery, vol. 38, no. 1, pp. 353-362, Feb. 2023.

[49] M. Sachs, D. L. Turcotte, J. R. Holliday and J. Rundle, "Forecasting Earthquakes: The RELM Test," in Computing in Science & Engineering, vol. 14, no. 5, pp. 43-48, Sept.-Oct. 2012.

[50] H. Aki, "Demand-Side Resiliency and Electricity Continuity: Experiences and Lessons Learned in Japan," in Proceedings of the IEEE, vol. 105, no. 7, pp. 1443-1455, July 2017.

[51] S. Shirakawa, "Engineering Education Examples for Electric Power Energy after the 2011 Large Disaster, and Power Energy Situation of Japan," 2020 23rd International Conference on Electrical Machines and Systems (ICEMS), Hamamatsu, Japan, 2020, pp.1111-1116.

[52] W. Shi, P. Zhuang and H. Liang, "Mobile Energy Resource Allocation for Distribution System Resilience Against Earthquakes," 2020 IEEE 92nd Vehicular Technology Conference (VTC2020-Fall), Victoria, BC, Canada, 2020, pp. 1-5.25

[53] A. Kuzmenko, D. Vorobyeva and E. Zolotukhin, "Monitoring the technical condition of dams of hydroelectric power plants with an automated monitoring and earthquake registration system," 2012 Power Engineering and Automation Conference, Wuhan, China, 2012, pp. 1-4.

[54] N. Malla, S. Poudel, N. R. Karki and N. Gyawali, "Resilience of electrical power delivery system in response to natural disasters," 2017 7th International Conference on Power Systems (ICPS), Pune, India, 2017, pp. 806-811.

[55] J. A. Weber, D. Wenzhong-Gao and J. Z. Zhai, "Case Study: Small-Scale Hybrid Integrated Renewable Energy System (HI-RES): Emergency Mobile Backup Power Generation Station," 2013 IEEE Green Technologies Conference (GreenTech), Denver, CO, USA, 2013, pp. 42-48.

[56] L. Tian and Z. Zhe, "Study on Earthquake Resistance of Electric Power System Based on System Reliability," 2010 International Conference on Intelligent System Design and Engineering Application, Changsha, China, 2010, pp. 437-440.

[57] F. De Caro and A. Vaccaro, "Review of Recent Trends in Power System Resilience-Oriented Decision-Making Methods," 2022 IEEE Power & Energy Society General Meeting (PESGM), Denver, CO, USA, 2022, pp. 1-5.

[58] Statista. (n.d.). Development of the number of earthquakes worldwide since 2000. Retrieved December 23, 2024, from [https://www.statista.com/statistics/263105/development-of-the number-of-earthquakes-worldwide-since 2000/]

[59] G. G. Amiri, A. Mahdavian, and F. M. Dana, "Attenuation relationships for Iran," *J. Earthq. Eng.*, vol. 11, no. 4, pp. 469–492, 2007

[60] M. Panteli, D. N. Trakas, P. Mancarella and N. D. Hatziargyriou, "Boosting the Power Grid Resilience to Extreme Weather Events Using Defensive Islanding," in IEEE Transactions on Smart Grid, vol. 7, no. 6, pp. 2913-2922, Nov. 2016

[61] S. Mishra and Y. S. Brar, "Load Flow Analysis Using MATLAB," 2022 IEEE International Students' Conference on Electrical, Electronics and Computer Science (SCEECS), BHOPAL, India, 2022, pp. 1-4.

[62] MATPOWER. (2023). *Case 24: IEEE Reliability Test System (RTS)*. MATPOWER 5.0 documentation. https://matpower.org/docs/ref/matpower5.0/case24_ieee_rts.html

[63] University of Washington Power Systems Test Case Archive. (n.d.). *Reliability Test System (RTS)*. Power Systems Test Case Archive. https://labs.ece.uw.edu/pstca/rts/pg_tcarts.htm

APPENDIX A

CODING SHEET

A) Code Section for Running Power Flow Analysis for IEEE-24 Bus System Under Normal Pre-Isolated Conditions.

```
clc
% Load Flow Analysis for IEEE-24 Bus System
% Add MATPOWER to path
addpath(genpath('/Users/aishat/Documents/MATLAB/matpower8.0/'));
savepath;
mpc = loadcase('case24_ieee_rts');

% Run Power Flow Analysis
results = runpf(mpc);
% Display Power Flow Results
if results.success
    fprintf('Load Flow Analysis Successful\n');
    % Display voltage magnitudes and angles for each bus
    fprintf('\nBus Voltages (p.u.) and Angles (degrees):\n');
    fprintf('-----------------------------------------\n');
    for i = 1:length(results.bus(:, 1))
        fprintf('Bus %d: Voltage = %.4f p.u., Angle = %.2f degrees\n', ...
            results.bus(i, 1), results.bus(i, 8), results.bus(i, 9));
    end

    % Display active and reactive power generated at each generator
    fprintf('\nGenerator Output (MW/MVAR):\n');
    fprintf('---------------------------------------\n');
    for i = 1:length(results.gen(:, 1))
        fprintf('Generator at Bus %d: P = %.2f MW, Q = %.2f MVAR\n', results.gen(i, 1), ...
            results.gen(i, 2), results.gen(i, 3));
    end

    % Display active and reactive power flows on each branch
    fprintf('\nBranch Power Flows (From/To):\n');
    fprintf('-----------------------------------------\n');
    for i = 1:length(results.branch(:, 1))
        fprintf('Branch %d (Bus %d -> Bus %d): P = %.2f MW, Q = %.2f MVAR\n', i, ...
            results.branch(i, 1), results.branch(i, 2), results.branch(i, 14), results.branch(i, 15));
    end
else
    error('Load Flow Analysis was unsuccessful.');
end

% Plot System Layout for Visualization
figure;
G = graph(mpc.branch(:, 1), mpc.branch(:, 2));
h = plot(G, 'Layout', 'force', 'NodeLabel', {});
title('IEEE 24-Bus System Layout');
highlight(h, mpc.gen(:, 1), 'NodeColor', 'g', 'MarkerSize', 8); % Highlight generator buses
xlabel('X Coordinate');
ylabel('Y Coordinate');
grid on;
```

B) Step by Step Demonstration on Code Section for Post-Isolation Analysis

---------- (1) Load MATPOWER & Basic Setup ---------- %% addpath(genpath('/Users/aishat/Documents/MATLAB/matpower8.0/'));

```
savepath;

mpc = loadcase('case24_ieee_rts');  % IEEE 24-bus system

% Bus-type column in MATPOWER bus matrix:
%  1=PQ, 2=PV, 3=Slack, 4=Isolated
BUS_TYPE = 2;
slack_buses = find(mpc.bus(:, BUS_TYPE) == 3);
disp(['Slack bus(es) identified: ', mat2str(slack_buses)]);

% Original network graph (for visualization/positions)
G_full = graph(mpc.branch(:,1), mpc.branch(:,2));
tmpPlot = plot(G_full, 'Layout','force', 'NodeLabel',{});
node_positions   = tmpPlot.XData;
node_positions_y = tmpPlot.YData;
x_limits = [min(node_positions)-0.5, max(node_positions)+0.5];
y_limits = [min(node_positions_y)-0.5, max(node_positions_y)+0.5];
close(gcf);
```

========== (2) Define Fragility & SRI Calculation ========== %% fragility_params = struct(...

```
    'slight_damage',    [0.4, 0.3], ...
    'moderate_damage',  [0.6, 0.3], ...
    'extensive_damage', [0.8, 0.3], ...
    'complete_damage',  [1.0, 0.3] );

calc_damage_probability = @(PGA, med, sig) normcdf(log(PGA/med)/sig);

compute_SRI_bus = @(PGA) ...
    ( 1*calc_damage_probability(PGA, fragility_params.slight_damage(1),    fragility_params.slight_damage(2)) + ...
      2*calc_damage_probability(PGA, fragility_params.moderate_damage(1),  fragility_params.moderate_damage(2)) + ...
      3*calc_damage_probability(PGA, fragility_params.extensive_damage(1), fragility_params.extensive_damage(2)) + ...
      4*calc_damage_probability(PGA, fragility_params.complete_damage(1),  fragility_params.complete_damage(2)) );
```

========== (3) Monte Carlo Simulation for Earthquakes (PGA) ========== %% num_scenarios = 10; % or more if you like

```
PGA_scenarios = zeros(1, num_scenarios);

for iSc = 1:num_scenarios
    rand_mag  = 5.0 + 2.0*rand();   % magnitude in [5,7]
    rand_dist = 10 + 90*rand();     % distance in [10,100] km
    soil_type = 'rock';             % or 'soft'

    PGA_scenarios(iSc) = ground_motion_model(rand_mag, rand_dist, soil_type);
end

disp('Random PGA values for each scenario:');
disp(PGA_scenarios);
```

========== (4) Prepare Arrays for Scenario Table ========== %% scenarioPGA = zeros(num_scenarios, 1);

```
scenarioSRI = zeros(num_scenarios, 1);
```

========== (5) Main Loop for Each Earthquake Scenario ========== %% for iSc = 1:num_scenarios

```
PGA_curr = PGA_scenarios(iSc);

% --- (A) Compute bus-level SRI & identify "vulnerable" buses
nBus = size(mpc.bus,1);
SRI_bus = zeros(nBus,1);
vulnerable_buses = [];
for b = 1:nBus
    SRI_bus(b) = compute_SRI_bus(PGA_curr);
    prob_complete = calc_damage_probability(PGA_curr, ...
                        fragility_params.complete_damage(1), ...
                        fragility_params.complete_damage(2));
    if prob_complete > 0.4
        vulnerable_buses = [vulnerable_buses; b];
    end
end
total_SRI = sum(SRI_bus);

% Exclude slack bus from "vulnerable" if you wish
old_vulnerable = vulnerable_buses;
vulnerable_buses = setdiff(vulnerable_buses, slack_buses);

% Print info
fprintf('\nScenario %d with PGA=%.4f:\n', iSc, PGA_curr);
fprintf('  Total System SRI = %.2f\n', total_SRI);
fprintf('  (Raw) Vulnerable Buses: %s\n', mat2str(old_vulnerable));
fprintf('  (Adjusted) Vulnerable Buses (excl. slack): %s\n', mat2str(vulnerable_buses));

% Store scenario-level results for final table
scenarioPGA(iSc) = PGA_curr;
scenarioSRI(iSc) = total_SRI;
```

```
% --- (B) Plot Pre-Isolation
figure('Name', sprintf('Scenario %d', iSc), 'NumberTitle','off');
subplot(1,2,1);
hPltPre = plot(G_full, 'XData',node_positions, 'YData',node_positions_y, 'NodeLabel',{});
highlight(hPltPre, vulnerable_buses, 'NodeColor','r','MarkerSize',8);
xlim(x_limits); ylim(y_limits);
title(sprintf('Pre-Isolation (Scenario %d)', iSc));

% --- (C) Build Weighted Graph for Spectral Clustering
f = mpc.branch(:,1);
t = mpc.branch(:,2);
G_spectral = graph(f, t);

% Default weights = 1
edge_weights = ones(G_spectral.numedges,1);
% If edge touches a vulnerable bus => smaller weight => likely cut
for e = 1:G_spectral.numedges
    ends = G_spectral.Edges.EndNodes(e,:);
    if any(ismember(ends, vulnerable_buses))
        edge_weights(e) = 0.3;  % e.g., 0.3
    end
end
G_spectral.Edges.Weight = edge_weights;

% Simplify => no parallel edges or loops => adjacency(...,'weighted') works
G_spectral = simplify(G_spectral, 'sum');

% Weighted adjacency & Laplacian
W = adjacency(G_spectral, 'weighted');
d = sum(W,2);
Lw = diag(d) - W;

[eigVecs, ~] = eigs(Lw, 2, 'smallestabs');
cluster_labels = kmeans(eigVecs, 2);
```

```
islandA = find(cluster_labels == 1);
islandB = find(cluster_labels == 2);
fprintf('  -> Spectral partition: IslandA=%s, IslandB=%s\n', ...
        mat2str(islandA), mat2str(islandB));

% --- (D) Cut ONLY inter-island lines => parted network
mpc_islanded = mpc;  % copy
to_remove = false(size(mpc.branch,1),1);
for br = 1:size(mpc.branch,1)
    ff = mpc.branch(br,1);
    tt = mpc.branch(br,2);
    inA_f = ismember(ff, islandA);
    inA_t = ismember(tt, islandA);
    if (inA_f && ~inA_t) || (~inA_f && inA_t)
        to_remove(br) = true;
    end
end
mpc_islanded.branch(to_remove,:) = [];
```

```
    % --- (E) Plot the Real Post-Isolation Network
    subplot(1,2,2);
    if isempty(mpc_islanded.branch)
        plot(0,0,'k.');
        title('Post-Isolation: No Connected Lines');
        xlim([-1,1]); ylim([-1,1]);
    else
        G_post = graph(mpc_islanded.branch(:,1), mpc_islanded.branch(:,2));
        hPltPost = plot(G_post, 'XData',node_positions, 'YData',node_positions_y, 'NodeLabel',{});
        highlight(hPltPost, islandA, 'NodeColor',[0.2 0.8 0.2],'MarkerSize',8);
        highlight(hPltPost, islandB, 'NodeColor',[0.7 0.3 0.8],'MarkerSize',8);
        xlim(x_limits); ylim(y_limits);
        title('Post-Isolation: 2 Islands');
    end

    % --- (F) Handle multi-island PF by splitting into subcases
    disp('  -> Splitting parted network into islands & running PF...');
    all_islands = {islandA, islandB};  % 2 islands

    for islIdx = 1:numel(all_islands)
        subCaseBuses = all_islands{islIdx};
        if isempty(subCaseBuses), continue; end

        subMPC = create_subcase(mpc_islanded, subCaseBuses);
        if isempty(subMPC.branch)
            fprintf('  Island %d has no branches => skipping PF.\n', islIdx);
            continue;
        end

        fprintf('  Island %d (buses=%s): Running PF...\n', islIdx, mat2str(subCaseBuses'));
        subRes = runpf(subMPC);
        if subRes.success
            fprintf('    Island %d: PF successful!\n', islIdx);
            disp('    Bus Voltages:');
            fprintf('%-6s  %-10s  %-10s\n','Bus','V(pu)','Angle(deg)');
            for ib = 1:size(subRes.bus,1)
                fprintf('%-6d  %-10.4f  %-10.4f\n',...
                    subRes.bus(ib,1), subRes.bus(ib,8), subRes.bus(ib,9));
            end
        else
            fprintf('    Island %d: PF failed or diverged.\n', islIdx);
        end
    end

end  % end of scenario loop
```

```
%% ======================================================================
%% L O C A L   F U N C T I O N S  (Below the main function in same file)
%% ======================================================================
```

```
function PGA_val = ground_motion_model(M, R, soil_type)
% Example ground motion model
    coeffs = [-3.0, 0.5, -0.005];
    rawPGA = coeffs(1) + coeffs(2)*M - coeffs(3)*log(R);
    PGA_val = exp(rawPGA);
    if strcmpi(soil_type,'soft')
        PGA_val = PGA_val * 1.05;
    end
    PGA_val = max(min(PGA_val, 1.0), 0.05);
end

function subMPC = create_subcase(mpc_islanded, busList)
% CREATE_SUBCASE builds a smaller MATPOWER case with only "busList" buses.

    subMPC = mpc_islanded;

    % Keep only the relevant buses
    keepBusMask = ismember(subMPC.bus(:,1), busList);
    subMPC.bus = subMPC.bus(keepBusMask, :);

    % Keep only branches that connect two buses in busList
    keepBranchMask = ismember(subMPC.branch(:,1), busList) & ...
                     ismember(subMPC.branch(:,2), busList);
    subMPC.branch = subMPC.branch(keepBranchMask, :);

    % Keep only generators on these buses
    if isfield(subMPC, 'gen')
        keepGenMask = ismember(subMPC.gen(:,1), busList);
        subMPC.gen = subMPC.gen(keepGenMask, :);
    end

    % Ensure at least one slack bus
    BUS_TYPE = 2;
    slack_mask = (subMPC.bus(:, BUS_TYPE) == 3);
    if ~any(slack_mask)
        subMPC.bus(1, BUS_TYPE) = 3;
        fprintf('    [create_subcase] No slack bus found here, forcing bus %d to Slack.\n', ...
            subMPC.bus(1,1));
    end
end
```